Supplement to Invalid Proxies and Volatility Changes

Giovanni Angelini, Luca Fanelli, Luca Neri

This version: November 6, 2025

Extended Acknowledgements

This paper has been presented at the First VTSS Virtual Workshop for Junior Researchers in Time Series (April 2023), CEBA Talks (November 2023), UZH Seminars (November 2023), UEA Seminars, University of East Anglia (December 2023), the IAAE 2022 Annual Meeting Oslo (June 2023), the SEM 2023 Conference, Milan (July 2023), the CFE 2023 Conference, Berlin (December 2023), the SIdE-IWEEE 2024 Workshop, Bolzano (January 2024), the 2024 Econometrics Workshop in memory of Carlo Giannini, Pavia (September 2024), the Sailing the Macro 2024 Workshop, Ortigia-Siracusa (September 2024), the Villa Mondragone 2024 Time Series Symposium, Frascati (October 2024), the EC^2 2024 Conference, Amsterdam (December 2024), the ICEEE 2025 Workshop, Palermo (May 2025). We wish to thank Gianni Amisano, Andrea Bastianin, Emanuele Bacchiocchi, Jacopo Bonchi, Paolo Bonomolo, Ralph Brüggemann, Alessandro Casini, Efrem Castelnuovo, Gianluca Cubadda, Raffaella Giacomini, Madina Karamysheva, Damian Kozbur, Helmut Lütkepohl, Rustam Ibragimov, Mirela Miescu, Giuseppe Ragusa, Barbara Rossi, Masanobu Taniguchi, Tommaso Tornese, Lorenzo Trapani, Anton Skrobotov, Giovanni Urga, Rainer Winkelmann, and Michael Wolf for comments and suggestions on previous drafts.

Introduction

In this Supplement, we extend and complete the paper along several dimensions.

Section S.1 introduces some special matrices used in the paper. Section S.2 complements Proposition 1 with a corollary which clarifies that the only possible scenario where the dynamic causal effects of interest can be estimated consistently ignoring volatility shifts is when relative (normalized) responses are estimated and IRFs remain constant across volatility regimes (up to scale). Section S.3 discusses a specific, illustrative example of a just-identifed proxy-SVAR with a volatility shift under stability restrictions. This model can be regarded as a possible benchmark specification when information on stability restrictions is scant.

Section S.4 extends the identification and estimation approach discussed in the paper along two dimensions. Firstly, it considers the case where the number of volatility breaks is $M \geq 2$, resulting in $M+1$ volatilty regimes. Secondly, it explores QML estimation as an alternative to the CMD estimation approach discussed in the paper.

Section S.5 complements the Monte Carlo results presented in the paper, providing details on the design of the experiments. It briefly discusses how to indirectly assess the identifiability of the proxy-SVAR when the information from volatility shifts is suspected to be poor and provides simulation resultd for a DGP where the shift in volatility is determined by the changes in the impact of the target shocks on the variables as well as by changes of the relative variance of the structural shocks.

Section S.6 integrates the empirical analysis with numerous details and additional results not included in the main text due to space constraints.

Section S.7 summarizes proofs of propositions and corollaries presented in the paper.

Unless differently specified, hereafter all references - except those starting with 'S.' - refer to sections, assumptions, equations and results in the main paper.

S.1 Special matrices

In the paper and in what follows, we make use of the following matrices (Magnus and Neudecker, 1999): D_n is the n-dimensional duplication matrix ($D_n vech(A) = vec(A)$, A being an $n \times n$ matrix) and $D_n^+ := (D_n' D_n)^{-1} D_n$ is the Moore-Penrose generalized inverse of D_n. K_{ns} is the ns-dimensional commutation matrix ($K_{ns} vec(A) = vec(A')$, A being $n \times s$). We simply use K_n in place of K_{nn} when $n = s$. In the proof of propositions we often exploit the result: $D_n^+ N_n = D_n^+$, where $N_n := \frac{1}{2}(I_{n^2} + K_n)$.

Furthermore, we denote with $vecd(A)$ the vector containing the diagonal elements of the square matrix A. Then, given the $p \times p$ diagonal matrix $A \equiv dg(A)$, the $p^2 \times p$ derivative $\mathcal{F}_A := \frac{\partial vec(A)}{\partial vecd(A)'}$ contains by construction '0' and '1'. Specifically, the matrix $\mathcal{F}_A$ is such that $rank[\mathcal{F}_A] = p$ if the diagonal elements of A are distinct. Conversely, $rank[\mathcal{F}_A] = p - p_1$ when there are p_1 repeated elements on the diagonal of A. Finally, we often use diag(A, B) to indicate a block diagonal matrix with blocks A and B on the main diagonal.

S.2 More on the estimation of target IRFs ignoring volatility shifts

In this section, we complement the results in Section 2.3. In particular, the following corollary specializes the result in Proposition 1 to the scenario where the volatility shift is not caused by changes in the on-impact coefficients ($\Delta_{H_{\bullet 1}} = 0_{n \times k}$). This scenario represents a common assumption in the classical identification-through-heteroskedasticity approach, where the change in volatility is ascribed solely to variations in the variances of the structural shocks.

Corollary 1 (Probability limit of $\hat{\Sigma}_{u,z}$ with $\Delta^{(0)}_{H_{\bullet 1}} = 0_{n \times k}$) *Under the same conditions as Proposition 1, with $\Delta^{(0)}_{H_{\bullet 1}} = 0_{n \times k}$ in (12):*

(i) $\hat{\Sigma}_{u,z} \xrightarrow{\mathbb{P}} \left[\tau_B^{(0)} H_{\bullet 1}^{(0)} + \left(1 - \tau_B^{(0)}\right) H_{\bullet 1}^{(0)} \left(\Lambda_{\bullet 1}^{(0)}\right)^{1/2}\right] \left(\Phi^{(0)}\right)'$;

(ii) for $k = 1$, $\hat{\Sigma}_{u_2,z} / \hat{\Sigma}_{u_1,z}^{-1} \xrightarrow{\mathbb{P}} H_{2,1}^{rel,(0)}$.

According to Corollary 1, the covariance matrix estimator $\hat{\Sigma}_{u,z}$ can be used to consistently estimate the target IRFs on the entire estimation sample only when two specific conditions are met: (i) responses remain constant across the two volatility regimes; (ii) the analysis focuses on relative responses obtained by imposing unit effect normalizations (see, e.g., Stock and Watson, 2018) rather than absolute responses.

Interestingly, Corollary 1.(ii) provides a theoretical rationale for some of the findings reported in Schlaak, Rieth, and Podstawski (2023), primarily obtained through simulation

studies. Corollary 1 highlights that incorporating the moment conditions implied by a shift in volatility into a framework where consistent estimation of the target IRFs is already achievable, can only enhance estimation precision (see also Carriero, Marcellino, and Tornese, 2024). This insight underscores the potential benefits of leveraging information from volatility shifts, even when consistent estimation is possible without it.

S.3 Stability restrictions: an extensive example

This section offers an example clarifying the notation for stability restrictions and illustrates the flexibility of the suggested approach. This example is meant to provide a potential (non-unique) starting point for practitioners when the placement of these restrictions is not immediately obvious.

Example 1 *Consider a proxy-SVAR that satisfies Assumptions 1-2 with $n = 3$ variables in Y_t and a single external instrument for the target shock $\varepsilon_{1,t} := \varepsilon^{(1)}_{1,t}$ ($r = k = 1$). Thus $\Phi = \varphi$ and $\Omega_{tr} = \omega$ are scalars. The system contains $n - k = 2$ non-target shocks, $\varepsilon_{2,t} := (\varepsilon^{(2)}_{1,t}, \varepsilon^{(2)}_{2,t})'$, so that $\Upsilon = (\upsilon_1, \upsilon_2)$ is 1×2; the elements υ_1 and υ_2 capture possible instrument contamination.*

Under a set of stability restrictions (see (18)), the structural matrices in the two volatility regimes are

$$G := \underbrace{\begin{pmatrix} h_{11} & h_{12} & h_{13} & 0 \\ h_{21} & h_{22} & h_{23} & 0 \\ h_{31} & h_{32} & h_{33} & 0 \\ \varphi & \upsilon_1 & \upsilon_2 & \omega \end{pmatrix}}_{\textit{vol. regime1}}, \qquad G + \Delta_G := \underbrace{\begin{pmatrix} h_{11} + \Delta_{h_{11}} & h_{12} & h_{13} & 0 \\ h_{21} + \Delta_{h_{21}} & h_{22} & h_{23} & 0 \\ h_{31} + \Delta_{h_{31}} & h_{32} & h_{33} & 0 \\ \varphi + \Delta_{\varphi} & \upsilon_1 & \upsilon_2 & \omega \end{pmatrix}}_{\textit{vol. regime2}} \tag{S.1}$$

$$\Psi : = \underbrace{\begin{pmatrix} 1 & & & \\ & \psi_2 & & \\ & & \psi_3 & \\ & & & \psi_4 \end{pmatrix}}_{\textit{change of relative variances in } \xi_t}. \tag{S.2}$$

Zeros in the last column of G and $G+\Delta_G$ reflect the proxy exclusion restriction: instrument measurement error has no contemporaneous impact on Y_t. Empty spaces in the specified Ψ stand for zeros. For $i, j = 1, 2, 3$, h_{ij} is the (i, j) element of H, and $\Delta_{h_{ij}}$ and Δ_{φ} are the parameters allowed to shift between regimes. Under the order condition in Proposition 2.(ii), υ_1 and υ_2 remain unrestricted, so instrument contamination is permitted. Finally, the diagonal elements ψ_2, ψ_3, ψ_4 capture the relative variance changes in the non-target shocks and measurement error ζ_t when the economy moves to the second volatility regime.

The restrictions on Ψ are obtained by specifying S_Ψ and s_Ψ in (18) as follows:

$$vecd(\Psi) = \underbrace{\begin{pmatrix} 0 & 0 & 0 \\ 1 & 0 & 0 \\ 0 & 1 & 0 \\ 0 & 0 & 1 \end{pmatrix}}_{S_\Psi} \underbrace{\begin{pmatrix} \psi_2 \\ \psi_3 \\ \psi_4 \end{pmatrix}}_{\psi} + \underbrace{\begin{pmatrix} 1 \\ 0 \\ 0 \\ 0 \end{pmatrix}}_{s_\Psi}$$

so that $c = \dim(\psi) = 3$. The restrictions on G are obtained similarly but the matrices S_G and s_G in (18) are of large dimensions and therefore omitted for space. The restrictions on Δ_G are obtained by specifying S_{Δ_G} and s_{Δ_G} in (18) as follows:

$$vec(\Delta_G) = S_{\Delta_G} \underbrace{\begin{pmatrix} \Delta_{h_{11}} \\ \Delta_{h_{21}} \\ \Delta_{h_{31}} \\ \Delta_\varphi \end{pmatrix}}_{\delta}$$

with S_{Δ_G} 16×4 selection matrix having one in the first 4 rows and zeros elsewhere and $s_{\Delta_G} = 0_{16\times 1}$.

Example 1 depicts a proxy-SVAR that is exactly identified and respects the rank condition in Proposition 2. The structural matrices G (γ), Δ_G (δ), and Ψ (ψ) contain a total of $a + b + c = 20$ unrestricted, non-zero elements. These parameters can be recovered uniquely from the reduced form information because the two regime-specific covariance matrices, $\Sigma_{\eta,1}$ and $\Sigma_{\eta,2}$, provide

$$(n + r)(n + r + 1)/2 \;=\; 4 \times 5/2 \;=\; 10$$

distinct second-moment equations per regime, i.e. $2 \times 10 = 20$ equations in all, exactly matching the number of unknowns.

Imposing one extra restriction makes the system over-identified and therefore testable. For instance, $\upsilon_2 = 0$ (orthogonality of the instrument z_t to the non-target shock $\varepsilon^{(2)}_{2,t}$) or $\Delta_\varphi = 0$ (constancy of instrument relevance across regimes) each supplies an additional equation that can be subjected to an over-identification test (adjusted for the regime break).

The volatility shift is explained by two mechanisms: (i) changes in the impact of the target shock on the endogenous variables, captured by the coefficients $\Delta_{h_{11}}, \Delta_{h_{21}}, \Delta_{h_{31}}$, and (ii) changes in the variances of the non-target shocks and the instrument's measurement error, captured by the elements of the vector ψ.

Interestingly, whenever $\Delta_\varphi \neq 0$, a change in instrument relevance also contributes to the volatility shift. The value 1 in the $(1, 1)$ element of Ψ implies that the variance of the target shock itself is unchanged across regimes; hence only the altered propagation of that shock drives the volatility shift. For normalized IRFs this is inconsequential, because such IRFs are identified only up to scale. If the instrument is contaminated, $\Upsilon := (\upsilon_1, \upsilon_2) \neq (0, 0)$, its variance equals $\varphi^2 + \upsilon_1^2 + \upsilon_2^2 + \omega^2$ in the first regime and $(\varphi + \Delta_\varphi)^2 + \upsilon_1^2\psi_2 + \upsilon_2^2\psi_3 + \omega^2\psi_4$ in the second, implying a regime-dependent correlation with both target and non-target shocks.

Aside from the VAR dynamics, the parameters needed to recover the target IRFs (13) in Example 1 are stacked in

$$\theta := (h_{11}, h_{21}, h_{31}, \Delta_{h_{11}}, \Delta_{h_{21}}, \Delta_{h_{31}})'.$$

All remaining (nuisance) parameters are nevertheless point-identified and can be estimated jointly with θ. Example 1 therefore illustrates that, even with two non-target shocks ($n - k = 2$), no restriction on $H_{\bullet 2}$ is required for identification. The stability restrictions further assume that the impact of non-target shocks is constant across volatility regimes. Equation (S.2) shows that, so long as ψ_2 and ψ_3 differ from 1, the non-target shocks affect the volatility shift only through changes in their relative variances: a deliberately neutral stance for nuisance parameters and fully consistent with the partial-identification logic of proxy-SVARs. At the same time, the empirical application demonstrates that the framework is flexible: when credible prior information is available, one can impose additional identifying constraints on both $H_{\bullet 2}$ and $\Delta_{H_{\bullet 2}}$ within the same stability restrictions template (18).

Example 1 offers a practical template for researchers who are unsure how to impose stability restrictions ex ante. In principle, just-identified models similar to that in Example 1 can be estimated, subsequently determining which parameters can be set to zero (especially those in Δ_G) based on the estimation results. This exercise can then be repeated heuristically, starting from different just-identified initial model configurations, until a plausible, parsimonious, non-rejected representation is achieved. However, since this procedure relies on sequential specification tests, the risk of introducing pre-testing bias can be substantial.

S.4 Multiple volatility regimes and QML estimation

This section extends the identification and estimation approach discussed in the paper along two dimensions: first, considering the case where the are at least two changes in volatility ($M \geq 2$) resulting in $M + 1$ volatility regimes (Section S.4.1), and second, QML estimation of the proxy-SVAR under stability restrictions (Section S.4.2).

S.4.1 Multiple volatility regimes

The reduced form proxy-SVAR model is the same as in equation (11), but now the parameters are allowed to change at the break points $T_{B_1}, \ldots, T_{B_M}$, where $1 < T_{B_1}, \ldots, < T_{B_M} < T$. Conventionally we assume that T_{B_0}:=1 and $T_{B_{M+1}}$:=T. The assumption that follows generalizes Assumptions 1-2 in the paper to a broader framework.

Assumption 3 *Given the proxy-SVAR (11),*
(i) the are M known *break points, $1 < T_{B_1} < \ldots < T_{B_M} < T$, such that $T_{B_1} \geq (n + r)$, $T_{B_i} - T_{B_{i-1}} \geq (n + r)$, $i = 2, \ldots, M + 1$, $(n + r) := dim(W_t)$;*
(ii) the law of motion of the autoregressive (slope) parameters $\pi(t)$:=$vec(\Gamma(t))$ and the

unconditional covariance matrix $\sigma_\eta(t)$:=$vech(\Sigma_\eta(t))$ *are given by:*

$$\pi(t)=\sum_{i=1}^{M+1}\pi_i\times\mathbb{I}\left(T_{B_{i-1}}+1\leq t\leq T_{B_i}\right)\ ,\ \ t=1,...,T$$

$$\sigma_\eta(t)=\sum_{i=1}^{M+1}\sigma_{\eta,i}\times\mathbb{I}\left(T_{B_{i-1}}+1\leq t\leq T_{B_i}\right)\ ,\ \ t=1,...,T \tag{S.3}$$

where $\Sigma_{\eta,i}<\infty$, $i=1,...,M+1$ *and:*

$$\sigma_{\eta,i}:=vech(\Sigma_{\eta,i})\neq\sigma_{\eta,j}:=vech(\Sigma_{\eta,j})\quad for\ \ i\neq j.$$

(iii) the process $\{\eta_t\}$, *where* $\eta_t:=(u_t',z_t')'$, *is* α*-mixing and has absolutely summable cumulants up to order eight on the* $M+1$ *volatility regimes.*

The relationships between the VAR disturbances and proxies and the structural shocks and measurement errors is given by $u_t=G(t)\xi_t$, where ξ_t is normalized to have unit variance across the $M+1$ volatility regimes (hence matrices Ψ_i are set to the identity for $i=2,...,M+1$), and $G(t)$ is defined by:

$$G(t):=G+\sum_{i=2}^{M+1}\Delta_{G_i}\times\mathbb{I}\left(T_{B_{i-1}}+1\leq t\leq T_{B_i}\right)\ ,\ \ t=1,...,T. \tag{S.4}$$

In (S.4), $\Delta_{G_i}:=G^{(i)}-G^{(i-1)}$, $i=2,...,M+1$ ($G^{(1)}:=G$) are $(n+r)\times(n+r)$ matrices. In (S.4), G contains the nonzero structural parameters before any break occurs, while the nonzero elements in the matrices Δ_{G_i} $i=2,...,M+1$ describe how and to what extent the instantaneous impact of the structural shocks changes across volatility regimes.

The mapping between the reduced- and structural-form parameters is now given by:

$$\Sigma_{\eta,1}=GG'\quad,\quad\Sigma_{\eta,i}=\left(G+\sum_{j=2}^{i}\Delta_{G_j}\right)\left(G+\sum_{j=2}^{i}\Delta_{G_j}\right)'\quad,\quad i=2,...,M+1 \tag{S.5}$$

and the linear identifying restrictions characterizing G and Δ_{G_i}, $i=2,\ldots,M+1$, can be collected in the expression:

$$\begin{pmatrix} vec(G)\\ vec(\Delta_{G_2})\\ \vdots\\ vec(\Delta_{G_{M+1}})\end{pmatrix}=\underbrace{\begin{pmatrix} S_G & & \cdots & \\ & S_{\Delta_{G_2}} & \cdots & \\ & & \ddots & \vdots\\ & & & S_{\Delta_{G_{M+1}}}\end{pmatrix}}_{S^*}\begin{pmatrix}\gamma\\ \delta_2\\ \vdots\\ \delta_{M+1}\end{pmatrix}. \tag{S.6}$$

In (S.6), γ is the $a\times1$ vector ($a=\dim(\gamma)$) that collects the free (unrestricted) elements in the matrix G, and δ_i is the $b_i\times1$ vector ($b_i=\dim(\delta_i)$) containing the free elements in the matrices Δ_{G_i}, $i=2,...,M+1$. The selection matrices S_G, s_G, $S_{\Delta_{G_2}}$ and $s_{\Delta_{G_2}}$ are of conformable dimensions and have obvious interpretation. To simplify notation, the "big" selection matrix in system (S.6) is summarized in the $(M+1)(n+r)\times(a+b_2+\ldots+b_{M+1})$

matrix S^*.

Given the proxy-SVAR in Assumptions 1-2, consider the moment conditions in (19) where G, Δ_G and Ψ are restricted as in (18). Assume $\varsigma_0 \in \mathcal{P}_\varsigma$ is a regular point of $\mathcal{J}(\varsigma) := \partial m(\sigma_\eta, \varsigma)/\partial \varsigma'$.

PROPOSITION S.1 (IDENTIFICATION UNDER CHANGING IRFS, $M+1$ REGIMES) *Given the proxy-SVAR in Assumptions 2–3, consider the moment conditions in (19) where G, Δ_{G_i} for $i = 2, ..., M+1$ are restricted as in (S.6) and set $\Psi = I_{n+r}$. Consider $\varsigma := (\gamma', \delta_2', ..., \delta_{M+1}')'$. Assume $\varsigma_0 \in \mathcal{P}_\varsigma$ is a regular point of $\mathcal{J}(\varsigma) := \partial m(\sigma_\eta, \varsigma)/\partial \varsigma'$. Then, irrespective of proxy properties:*

(i) *a necessary and sufficient condition for the (local) identification of ς_0 is that $rank[\mathcal{J}(\varsigma)] = a + b_2 + ... + b_{M+1}$ in a neighborhood of ς_0, where $\mathcal{J}(\varsigma_0)$ is the $(1/2)(M+1)(n+r)(n+r+1) \times (a + b_2 + ... + b_{M+1})$ Jacobian evaluated at ς_0, $\mathcal{J}(\varsigma_0) := \mathcal{J}(\varsigma)|_{\varsigma=\varsigma_0}$, with*

$$\mathcal{J}(\varsigma) = 2(I_{M+1} \otimes D_{n+r}^+)\, \mathcal{H}_{M+1}(\varsigma)\, S^* \tag{S.7}$$

where

$$\mathcal{H}_{M+1}(\varsigma) = \begin{pmatrix} (G \otimes I_{n+r}) & 0_{(n+r)^2 \times (n+r)^2} & \cdots & 0_{(n+r)^2 \times (n+r)^2} \\ (G + \Delta_{G_2}) \otimes I_{n+r} & (G + \Delta_{G_2}) \otimes I_{n+r} & \cdots & 0_{(n+r)^2 \times (n+r)^2} \\ \vdots & \vdots & \ddots & \vdots \\ \left(G + \Delta_{G_{M+1}}\right) \otimes I_{n+r} & \left(G + \Delta_{G_{M+1}}\right) \otimes I_{n+r} & \cdots & \left(G + \Delta_{G_{M+1}}\right) \otimes I_{n+r} \end{pmatrix}.$$

(ii) A necessary order condition is:

$$(a + b_2 + \ldots + b_{M+1}) \leq (M+1)\,(n+r)(n+r+1)/2.$$

Note that for $M = 1$, Proposition S.1 collapses to Proposition 2 in the paper. Proposition S.1 can be extended to unrestricted (multiple) Ψ with appropriate adjustments to ς, S^*, and $\mathcal{H}_{M+1}(\varsigma)$.

When the necessary and sufficient rank condition in Proposition S.1 is satisfied, the proxy-SVAR can be estimated by extending the CMD approach discussed in the paper to the multiple volatility regimes case. We refer to Bacchiocchi and Kitagawa (2025) for discussion about SVARs in which identification is local and not global.

S.4.2 QML ESTIMATION

To simplify exposition, in the remainder of this section we consider quasi-maximum likelihood estimation based on observations:

$$W_{-l+1}, W_{-l+2}, ..., W_0, W_1, ..., W_T$$

for the case of a single break ($M = 1$) occurring at the known date $t = T_B$, i.e. two volatility regimes in the data. The generalization to the case $M \geq 2$ is tedious but straightforward. Hence, given the reduced form model (11), the QML estimation for the whole sample, $W_1, ..., W_T$, conditional on $W_{-l+1}, W_{-l+2}..., W_0$, based on the assumption of conditionally

Gaussian errors, is given by maximization of

$$\prod_{i=1}^{M+1} \prod_{t=T_{B_{i-1}}+1}^{T_{B_i}} f(W_t \mid W_{t-1}, ..., W_{t-l}; \Gamma_i, \Sigma_{\eta,i})$$

where

$$\begin{aligned} &f(W_t \mid W_{t-1}, ..., W_{t-l}; \Gamma_i \, , \Sigma_{\eta,i}) \\ &\quad = \frac{1}{(2\pi \det(\Sigma_{\eta,i}))^{1/2}} \exp\left\{ -\frac{1}{2} \left[W_t - \Gamma_i X_t\right]' \Sigma_{\eta,i}^{-1} \left[W_t - \Gamma_i X_t\right] \right\}. \end{aligned}$$

By standard manipulations, and conventionally denoting with $\mathring{G} = G(\gamma)$ and $\mathring{\Delta}_G = \Delta_G(\delta)$ the counterparts of the matrices G and Δ_G that satisfy the identification conditions in Proposition 2, the concentrated, quasi-Gaussian log-likelihood of the proxy-SVAR reduces to:

$$\begin{aligned} \log L_T(\varsigma) \quad = \quad & const - \tfrac{T_B}{2} \log \left|\mathring{G}\right|^2 - \tfrac{T-T_B+1}{2} \log \left|\mathring{G} + \mathring{\Delta}_G\right|^2 \\ & -\tfrac{T_B}{2} tr\left(\mathring{G}^{-1} \left(\mathring{G}^{-1}\right)' \hat{\Sigma}_{\eta,1}\right) \\ & -\tfrac{T-T_B+1}{2} tr\left(\left(\left(\mathring{G} + \mathring{\Delta}_G\right)^{-1}\right)' \left(\mathring{G} + \mathring{\Delta}_G\right)^{-1} \hat{\Sigma}_{\eta,2}\right), \end{aligned} \tag{S.8}$$

where $\hat{\Sigma}_{\eta,1}$ and $\hat{\Sigma}_{\eta,2}$ are estimates of the reduced form covariance matrices obtained from the two volatility regimes. Bacchiocchi and Fanelli (2015) discuss the derivation of the score and associated information matrix for a case analogous to the quasi-likelihood function in (S.8).

S.5 Further Monte Carlo results

This section provides further details about the Monte Carlo experiments presented in the paper. It presents also additional simulation results. Specifically, the focus in on (i) the design of the experiments analyzed in the main text, (ii) the measure of relative performance used for comparisons with other methods, (iii) the role that the estimation of the smallest singular value of the Jacobian matrix $\mathcal{J}(\varsigma)$ (see Proposition 2) plays in detecting, ex-post, situations where shifts in volatility provide limited information for identification and, finally, (iv) the combined effect of changes in the on-impact effects of the shocks on the variables and changes in the relative variance of the shocks.

(i) Design of the experiment The design of the experiment is as follows. We generate pseudo-samples of length T from a bivariate ($n = 2$) stable VAR(1) with zero initial values ($Y_0 := 0_{2\times 1}$), and a single break in the unconditional covariance matrix occurring at the break date $T_B := \lfloor 0.5T \rfloor$, i.e. located at the middle of the overall sample. The DGP matrix

of autoregressive parameters (see (8)) is given by:

$$\Pi := \begin{pmatrix} 0.825 & 0.5 \\ -0.2 & 0.75 \end{pmatrix}$$

and its largest eigenvalue in modulus is equal to 0.84, a persistence that aligns with the level we observe in empirical analyses. Given the vector of structural shocks, $\varepsilon_t := (\varepsilon_{1,t}, \varepsilon_{2,t})'$, $\varepsilon_{1,t}$ is the target structural shock ($\varepsilon_{2,t}$ the non-target shock), which is instrumented by the proxy z_t ($r = k = 1$). The DGP for the instrument z_t is described by the linear measurement error model:

$$\begin{aligned} z_t &= \left[\varphi + \Delta_\varphi \cdot \mathbb{I}\left(t \geq T_B + 1\right)\right] \varepsilon_{1,t} + \left[\upsilon + \Delta_\upsilon \cdot \mathbb{I}\left(t \geq T_B + 1\right)\right] \varepsilon_{2,t} \\ &\quad + \left[\omega + \Delta_\omega \cdot \mathbb{I}\left(t \geq T_B + 1\right)\right] \zeta_t, \qquad t = 1, ..., T \end{aligned}$$

where φ and $\varphi + \Delta_\varphi$ are the relevance parameters, υ, $\upsilon + \Delta_\upsilon$ the contamination parameters, whose nonzero values capture the connections of the instrument with the non-target shock. Finally, ω is the standard deviation of the proxy's measurement error ζ_t. In this design, also the variance of the measurement error may changes from ω^2 to $(\omega + \Delta_\omega)^2$ in the shift from the first to the second volatility regime. Relevance and exogeneity/contamination are captured by the correlations:

$$corr(z_t, \varepsilon_{1,t}) = \begin{cases} \frac{\varphi}{(\varphi^2+\upsilon^2+\omega^2)^{1/2}}, & t \leq T_B, \\ \frac{\varphi+\Delta_\varphi}{((\varphi+\Delta_\varphi)^2+(\upsilon+\Delta_\upsilon)^2+(\omega+\Delta_\omega)^2)^{1/2}}, & t \geq T_B + 1 \end{cases}$$

$$corr(z_t, \varepsilon_{2,t}) = \begin{cases} \frac{\upsilon}{(\varphi^2+\upsilon^2+\omega^2)^{1/2}}, & t \leq T_B, \\ \frac{\upsilon+\Delta_\upsilon}{((\varphi+\Delta_\varphi)^2+(\upsilon+\Delta_\upsilon)^2+(\omega+\Delta_\omega)^2)^{1/2}}, & t \geq T_B + 1 \end{cases}.$$

We consider scenarios in which the external instrument satisfies the exogeneity condition ($\upsilon = 0, \upsilon + \Delta_\upsilon = 0$, implying $corr(z_t, \varepsilon_{2,t}) = 0$ for any t), and scenarios where it does not ($\upsilon \neq 0, \upsilon + \Delta_\upsilon \neq 0$). Similarly, we examine situations in which relevance is met, meaning that the correlation with the target shock is strong on the estimation sample, and scenarios in which the external instrument is local-to-zero as in Staiger and Stock (1997), i.e. $\varphi := cT^{-1/2}$, with $|c| < \infty$. In general, the design covers all possible instrument properties, see c.(i)-c.(iv), Section 2. The DGP values for φ, υ, ω and Δ_ω are specified below.

By combining the VAR with the external instrument for $\varepsilon_{1,t}$, the covariance matrices satisfy, under Assumption 1, the moment conditions:

$$\begin{aligned} \Sigma_{\eta,1} &= GG' \\ \Sigma_{\eta,2} &= (G + \Delta_G)\Psi(G + \Delta_G)' \end{aligned}$$

with DGP values for G, Δ_G and Ψ given by:

$$G = \begin{pmatrix} H_{\bullet 1} & H_{\bullet 2} & 0_{2\times 1} \\ \Phi & \Upsilon & \Omega_{tr} \end{pmatrix} = \begin{pmatrix} 1.00 & 0.40 & 0 \\ 0.70 & 0.90 & 0 \\ \varphi & \upsilon & 1 \end{pmatrix}$$

$$\Delta_G = \begin{pmatrix} \Delta_{H_{\bullet 1}} & \Delta_{H_{\bullet 2}} & 0_{2\times 1} \\ \Delta_\Phi & \Delta_\Upsilon & \Delta_{\Omega_{tr}} \end{pmatrix} := \begin{pmatrix} -0.50 & 0 & 0 \\ -1.00 & 0 & 0 \\ \Delta_\varphi & \Delta_\upsilon & -0.04 \end{pmatrix}$$
$$\Psi = I_3.$$

The true vector of structural parameters is $\varsigma^{(0)} := (\gamma_0', \delta_0')'$, with

$$\gamma_0 := (1, 0.7, 0.40, 0.90, \varphi_0, \upsilon_0, 1)' \quad \text{and} \quad \delta_0 := (-0.5, -1, \Delta_{\varphi,0}, \Delta_{\upsilon,0}, -0.040)'.$$

In this design, the target IRFs in (13) change across the two volatility regimes solely because of changes in the on-impact parameters $H_{\bullet 1} := (1, 0.7)'$, as captured by the elements in $\Delta_{H_{\bullet 1}} := (-0.5, -1)'$. Overall, the total number of structural parameters to estimate when $\upsilon \neq 0, \Delta_\upsilon \neq 0$ (instrument exogeneity fails) is 11, while there are $(n+r)(n+r+1)$ =12 moment conditions. Therefore, the proxy-SVAR incorporates one (d =1) testable overidentifying restriction when $\upsilon \neq 0, \Delta_\upsilon \neq 0$ (exogeneity fails), and three (d =3) testable overidentifying restrictions when $\upsilon = 0, \Delta_\upsilon = 0$ (instrument exogeneity holds) and the zero restrictions are imposed in estimation. The necessary and sufficient rank condition implied by Proposition 2 is satisfied for the specified values of $(\varphi_0, \Delta_{\varphi,0})$ and $(\upsilon_0, \Delta_{\upsilon,0})$ we consider below.

In all experiments, we generate N =10,000 samples of lengths $T = \{250,\ 500,\ 1,000\}$, respectively, under the hypothesis that the structural shocks $\varepsilon_t := (\varepsilon_{1,t}, \varepsilon_{2,t})'$ and the proxy's measurement error ζ_t are drawn from $iidN(0,1)$ processes.[1] When dealing with strong proxies, the DGP values of φ and Δ_φ are such that $corr(\varepsilon_{1,t}, z_t) = 0.58$ for the full sample. Instead, when dealing with+ local-to-zero proxies, the correlations vary with the sample size, namely $corr(\varepsilon_{1,t}, z_t) = \{0.045, 0.0318, 0.0225\}$, depending on whether the sample length T is equal to 250, 500 or 1, 000 respectively.

(II) Measure of relative performance Table 1 in the main text summarizes measures of relative performance. These are based on Mean Squared Error (MSE) and are inspired by Schlaak et al. (2023). We explain how these measures are constructed.

For q≥ 2, we have:

$$rel\text{-}MSE^{Model.q}_{Model.1} := \tau_B \times rel\text{-}MSE^{Model.q}_{Model.1}(t)\mathbb{I}\left(t \leq T_B\right) + (1-\tau_B) \times rel\text{-}MSE^{Model.q}_{Model.1}(t)\mathbb{I}\left(t > T_B\right) \tag{S.9}$$

where $\tau_B := \lfloor T_B/T \rfloor$ is the fraction of the sample covering the first volatility regime and:

$$rel\text{-}MSE^{Model.q}_{Model.1}(t) := \frac{1}{25}\sum_{h=0}^{25-1}\left\{\frac{\frac{1}{N}\sum_{j=1}^{N}\left(\widehat{IRF}^{Model.q}_{i,1,j}(t,h) - IRF^0_{i,1}(t,h)\right)^2}{\frac{1}{N}\sum_{j=1}^{N}\left(\widehat{IRF}^{Model.1}_{i,1,j}(t,h) - IRF^0_{i,1}(t,h)\right)^2}\right\}. \tag{S.10}$$

In (S.9)-(S.10), N =10,000 is the number of Monte Carlo simulations (with j associated index), $i = \{1, 2\}$ denotes the response variable in $Y_t = (Y_{1,t}, Y_{2,t})'$, $IRF^0_{i,1}(t,h)$ is the true value of the absolute response of $Y_{i,t+h}$ to the target shock $\varepsilon_{1,t}$ (see equation (13)),

[1] We can relax both Gaussianity and the iid hypothesis provided the process $\eta_t := (u_t', z_t')'$ respects the α-mixing conditions stated in Assumption 1.

and $\widehat{IRF}_{i,1,j}^{Model.q}(t,h)$ the corresponding estimate obtained from Model.q on the sample of observation generated at the j-th DGP. The measures in (S.9)-(S.10) are opportunely adapted to considering the whole sample of length T for Model.4 and Model.5, where the target IRFs are kept constant across the two volatility regimes.

For $q \geq 2$, measures obtained from (S.9)-(S.10) greater than 1 indicate that Model.q performs worse in terms of MSE than the benchmark Model.1. Conversely, values less than 1 indicate that there are relative gains in performance.

(iii) Checks of identifiability and limited information from volatility shifts The results in Table 1 and Table 2 are obtained under scenarios in which the proxy-SVAR with a break in unconditional volatility is identified. Identifiability depends on the full column rank condition of the Jacobian matrix $\mathcal{J}(\varsigma)$, as derived in Proposition 2; see equation (20).

In practical situations, investigators can, in principle, test the rank of the Jacobian matrix ex-post, meaning after estimating the model and substituting the elements in G, Δ_G and Ψ in (20) with their estimates, obtaining $\mathcal{J}(\hat{\varsigma}_T)$. Tests of rank that can be applied in these cases are discussed in e.g. Al-Sadoon (2017); see also references therein.

In the empirical illustration discussed in Section 3, we assessed the quality of identification by inspecting the smallest singular value of the estimated Jacobian matrix $\mathcal{J}(\hat{\varsigma}_T)$. Specifically, we computed bootstrap confidence intervals for the smallest singular value, emphasizing that this process does not involve rigorous statistical inference. Now, we investigate whether such diagnostic checks are empirically plausible via Monte Carlo simulations.

We begin by considering the case where the change in VAR covariance matrices is sufficiently large to identify the model, consistent with the DGP considered thus far. Table S.1 summarizes the average estimated smallest singular value of the Jacobian matrix across Monte Carlo simulations, along with the associated interquartile ranges (IQRs). IQRs are used here as broad approximations of confidence intervals. We explore scenarios with both relevant and local-to-zero instruments, as well as both exogenous and contaminated instruments. The results in Table S.1 indicate that when the change in volatility is sufficiently strong for identification, the smallest singular values of the estimated Jacobian matrix are far from zero, and the associated IQRs do not include zero. Furthermore, Table S.1 shows that instrument properties do not affect the identifiability of the model, confirming the analytical results discussed in the paper and the results in Tables 1 and 2.

Our analysis proceeds by reexamining the performance of the stability restrictions approach under a different framework. In particular, to envisage how identification information stemming from the change in unconditional volatility may deteriorate and lead to identification failure, we notice that setting $\Psi := I_{n+r}$ (to simplify), the moment conditions (16) imply that the shift in volatility is entirely due to the nonzero elements in the matrix Δ_G:

$$\Sigma_{\eta,2} - \Sigma_{\eta,1} = G\Delta_G' + \Delta_G G' + \Delta_G \Delta_G'. \tag{S.11}$$

Recall that in (S.11), the nonzero entries in Δ_G (δ) capture changes in the parameters in the transition from the first to the second volatility regime. This raises the question of how large the magnitude of shifts in Δ_G (δ) must be in (S.11) for the approach outlined in the previous sections to remain valid. To characterize the phenomenon of "shrinking

covariance shift", we relax Assumption 1(iv) (while keeping all the other assumptions valid) and approximate Δ_G in (S.11) by the local-to-zero condition:

$$\Delta_G = \varrho_T \tilde{\Delta}_G \tag{S.12}$$

where ϱ_T is a scalar that converges to zero as the sample size increases, and $\tilde{\Delta}_G$ represents a re-scaled version of the matrix Δ_G that therefore fulfills the same stability restrictions as Δ_G in (18). According to (S.12), the magnitude of the change in volatility in the proxy-SVAR is controlled by the parameter $\varrho_T \to 0$, whose speed of convergence to zero plays a crucial role. Under (S.12), the distance between $\Sigma_{\eta,2}$ and $\Sigma_{\eta,1}$ in (S.11) can be written as:

$$\begin{aligned}\Sigma_{\eta,2} - \Sigma_{\eta,1} &= \varrho_T G \tilde{\Delta}_G' + \varrho_T \tilde{\Delta}_G G' + \varrho_T \tilde{\Delta}_G \varrho_T \tilde{\Delta}_G' \\ &= \varrho_T \underbrace{\left[G \tilde{\Delta}_G' + \tilde{\Delta}_G G' + \tilde{\Delta}_G \varrho_T \tilde{\Delta}_G' \right]}_{C_T}\end{aligned} \tag{S.13}$$

so that it is seen that, as in Bai (2000), $C_T \to C = (G\tilde{\Delta}_G' + \tilde{\Delta}_G G') \neq 0_{(n+r)\times(n+r)}$ and $(\Sigma_{\eta,2} - \Sigma_{\eta,1}) \to 0_{(n+r)\times(n+r)}$, as $\varrho_T \to 0$. Intuitively, given (S.13) and T being large, the moment conditions in system (16) no longer produce $(n+r)(n+r+1)$ independent moment conditions that offer meaningful information on the parameters ς. This could lead to the failure of the necessary and sufficient rank conditions for identification derived in Proposition 2.

By combining the conditions $\varrho_T \to 0$ with the stability restrictions (18), the implied Jacobian matrix now is:

$$\tilde{\mathcal{J}}(\varsigma) := 2\left(I_2 \otimes D_{n+r}^{+}\right) \begin{pmatrix} (G \otimes I_{n+r}) & 0_{(n+r)^2\times(n+r)^2} \\ (G + \tilde{\Delta}_G) \otimes I_{n+r} & (G + \tilde{\Delta}_G) \otimes I_{n+r} \end{pmatrix} \begin{pmatrix} S_G & 0 \\ 0 & \varrho_T S_{\Delta_G} \end{pmatrix}$$

and demonstrates that, even in cases where $\tilde{\mathcal{J}}(\varsigma)$ has full column rank for nonzero values of ϱ_T (no shrinking), identification fails as ϱ_T approaches zero.

Table S.2 summarizes the estimated smallest singular values of the Jacobian matrix and associated IQRs when VAR covariance matrices satisfy the conditions $(\Sigma_{\eta,2} - \Sigma_{\eta,1}) \to 0_{(n+r)\times(n+r)}$, as $\varrho_T \to 0$ and shrink at the rate $\varrho_T = O(T^{-1/2})$. It can be observed a departure from the patterns seen in Table S.1. In contrast to the scenarios presented in Table S.1, where the ratio between the estimated average smallest singular value and the average length of the IQRs consistently exceeds 2, we now observe a distinct trend. Specifically, when exogeneity is not imposed in the estimation, this ratio is systematically less than 2, regardless of instrument strength, indicating rank collapse of the Jacobian matrix $\mathcal{J}(\varsigma)$. Conversely, when instrument exogeneity is imposed in the estimation (regardless of its validity in the DGP), we do not observe rank collapse. This phenomenon arises because, when deviations from exogeneity are allowed, the instruments carry limited information about the non-target shocks under shrinking volatility shifts. Consequently, the limited identification information from the shifts in volatility extends to the entire system. In contrast, imposing instrument exogeneity prevents this information leakage. In this case, the only source of identification for the non-target shocks is the strong instruments.

We can argue that the results outlined in Tables S.1 and S.2 indirectly lend support to the indirect check of identifiability of the fiscal proxy-SVAR estimated in Section 3 of the

paper.

(iv) Additional simulation results The simulation above and the results discussed in Section 2.5 of the main text are based on a design where $\Psi = I_3$, implying that the relative variance of the structural shocks remain constant across volatility regimes. We relax this condition, providing additional Monte Carlo results based on a DGP where volatility shifts come from both changes in the instantaneous impact of structural shocks on variables and changes in their relative variance.

The DGP is similar to the one discussed in point (i) above. The main difference is that the moment conditions:

$$\begin{aligned} \Sigma_{\eta,1} &= GG' \\ \Sigma_{\eta,2} &= (G + \Delta_G)\Psi(G + \Delta_G)' \end{aligned}$$

are now based on the following population values of the matrices G, Δ_G and Ψ:

$$G = \begin{pmatrix} 1 & 0.4 & 0 \\ 0.7 & 0.9 & 0 \\ \varphi & \upsilon & 1 \end{pmatrix}, \qquad \Delta_G = \begin{pmatrix} 0 & 0 & 0 \\ -0.5 & 0 & 0 \\ \Delta_\varphi & 0 & 0 \end{pmatrix}, \qquad \Psi = \begin{pmatrix} \psi & 0 & 0 \\ 0 & 1 & 0 \\ 0 & 0 & 1 \end{pmatrix} \tag{S.14}$$

where ψ, which can be now different from 1, captures the variance of the target shock relative to the two non-target shocks in the system. We set the population value of this parameter to 0.8. It is now seen that the change in the unconditional covariance matrix is determined by changes in the impact of the target shocks on the variables (first column of Δ_G), as well as by a change in the relative variance of the target shock (the (1,1) element of Ψ). The zero restrictions in G and Δ_G, and the $(2,2)$ and $(3,3)$ elements of Ψ, are assumed known by the econometrician and correctly imposed in estimation. With $\upsilon \neq 0$ (instrument contamination allowed), the specified proxy-SVAR with shift in volatility features 12 moment conditions for 10 free parameters. The model satisfies the necessary and sufficient rank condition in Proposition 2, therefore it is overidentified and testable.

Again, we consider scenarios in which the external instrument satisfies the exogeneity condition ($\upsilon = 0, \upsilon + \Delta_\upsilon = 0$, implying $corr(z_t, \varepsilon_{2,t}) = 0$ for any t), and scenarios where it does not ($\upsilon \neq 0, \upsilon + \Delta_\upsilon \neq 0$). Similarly, we examine situations in which relevance is met, meaning that the correlation with the target shock is strong on the estimation sample, and scenarios in which the external instrument is local-to-zero. Estimation is carried out by the CMD approach.

Estimation accuracy across the five methods discussed in Section 2.5 is summarized in Table S.3. This table mirrors the information in Table 1. The evidence from Table S.3 aligns with the findings already commented in the main text for the DGP based on $\Psi = I_3$.

We complete our analysis by checking the performance of the overidentifying restrictions test in this DGP. Table S.4 summarizes the rejection frequencies of the overidentifying restrictions test when the relative variance ψ is incorrectly restricted to 1 (ascribing, therefore, the shift in the covariance matrix solely to changes in the instantaneous impact of the target shock on the variables) and when it is left unrestricted in estimation. Testing results in the left-side of Table S.4 suggest that the test displays reasonable power (increasing with the sample size) also in the presence of a specification that features relatively small

departures from the DGP; on the other hand, results on the right-side of Table S.4 confirm that size is under control when stability restrictions are correctly specified.

S.6 Further empirical results

In this section, we complement the empirical analyses presented in the paper with additional results. Specifically, we: (i) define the fiscal multipliers; (ii) discuss the specification of the baseline proxy-SVAR estimated while ignoring the volatility break; (iii) present some diagnostic results on the reduced form fiscal VAR; (iv) detail estimation procedures and simple checks of model identifiability; (v) comment on the inferred dynamic tax multipliers; (vi) plot the IRFs from the baseline model's estimation and compare them with results in Mertens and Ravn (2014); (vii) extend the model by including consumer price inflation in the system; (viii) summarize the estimated fiscal spending multipliers; (ix) discuss results on the fiscal-spending multiplier.

(i) Fiscal multipliers Let P_t represent either the level of fiscal spending or the level of tax revenues (not in logs), and GDP_t^e denote the unlogged level of output. For simplicity, we use β_{y_h} to denote the response of log-output at horizon h to a one-standard deviation fiscal policy shock, and β_{p_0} for the on-impact response of the logged fiscal variable to the corresponding one-standard deviation fiscal policy shock. Then, in our context, dynamic multipliers, defined as the dollar response of output to an effective change in the fiscal variable of 1 dollar occurred h period before, are given by:

$$\mathcal{M}_{p,h} := (\beta_{y_h}/\beta_{p_0}) \times Scaling_p \tag{S.15}$$

where $Scaling_p$ is a policy shock-specific scaling factor converting elasticities to dollars. We set the scaling factor equal to the sample means of the series (GDP_t^e/P_t) computed over the estimation period. Thus, when in the paper we deal with the volatility change and the stability restriction approach, the scaling factor is calculated considering observations in the corresponding volatility regimes. We refer to Caldara and Kamps (2017) and Angelini, Caggiano, Castelnuovo, and Fanelli (2023) for a detailed discussion.

(ii) Specification with no shift in volatility The proxy-SVAR is estimated over the whole sample period 1950:Q1-2006:Q4, under the assumption that the fiscal instruments z_t are relevant and exogenous for the target fiscal shocks $\varepsilon_{1,t} := (\varepsilon_t^{tax}, \varepsilon_t^g)'$. We consider the following specification:

$$\begin{pmatrix} u_t^{TR} \\ u_t^{GS} \\ u_t^{GDP} \end{pmatrix} = \underbrace{\begin{pmatrix} h_{1,1} & h_{1,2} \\ h_{2,1} & h_{2,2} \\ h_{3,1} & h_{3,2} \end{pmatrix}}_{H_{\bullet 1}} \underbrace{\begin{pmatrix} \varepsilon_t^{tax} \\ \varepsilon_t^g \end{pmatrix}}_{\varepsilon_{1,t}} + H_{\bullet 2} \underbrace{\varepsilon_t^y}_{\varepsilon_{2,t}} \tag{S.16}$$

$$\underbrace{\begin{pmatrix} z_t^{tax} \\ z_t^g \end{pmatrix}}_{z_t} = \underbrace{\begin{pmatrix} \varphi_{1,1} & \varphi_{1,2} \\ 0 & \varphi_{2,2} \end{pmatrix}}_{\Phi} \underbrace{\begin{pmatrix} \varepsilon_t^{tax} \\ \varepsilon_t^g \end{pmatrix}}_{\varepsilon_{1,t}} + \underbrace{\begin{pmatrix} \tilde{\zeta}_t^{tax} \\ \tilde{\zeta}_t^g \end{pmatrix}}_{\tilde{\zeta}_t} \tag{S.17}$$

where the zero restriction in the (2,1) element of Φ is sufficient for identification (Angelini and Fanelli, 2019). The zero in the (2,1) position of the matrix Φ in (S.17) posits that the fiscal spending proxy solely instruments the fiscal spending shock. In turn, we permit the tax proxy to possibly convey information on the fiscal spending shock other than the tax shock, allowing the data to inform on the significance of the parameter $\varphi_{1,2}$. Then we estimate the model by the CMD approach. In (S.16)-(S.17), $\tilde{\zeta}_t := (\tilde{\zeta}_t^{tax}, \tilde{\zeta}_t^{g})'$ denotes the vector of (unnormalized) measurement errors associated with the two fiscal proxies.

(III) VAR DIAGNOSTICS In Section 3 we estimate a VAR for $Y_t := (TR_t, GS_t, GDP_t)'$ and two proxies $z_t := (z_t^{tax}, z_t^{g})'$. The VAR residuals $\hat{u}_t = (\hat{u}_t^{TR}, \hat{u}_t^{GS}, \hat{u}_t^{GDP})'$, $t = 1, ..., T$ and the two fiscal proxies z_t, $t = 1, ..., T$ are plotted over the sample period 1950:Q1-2006:Q4 in the left and right columns of Figure S.1, respectively. Standard residual-based diagnostic tests (available upon request), indicate that the VAR disturbances are serially uncorrelated but exhibit conditional heteroskedasticity. The graphs of the VAR residuals clearly show a reduction in variability beginning in the early 1980s. The estimated break point (Bai, 2000) corresponds to the vertical lines in Figure S.1.

(IV) ESTIMATION The proxy-SVAR specified in (24) involves $(a + b) = 27$ parameters (those in the matrices G and Δ_G in (24)), collected in the vector ς, and is based on $(n+r)(n+r+1) = 30$ moment conditions provided by the VAR error covariance matrices $\Sigma_{\eta,2}$ and $\Sigma_{\eta,1}$, respectively. The model is overidentified if the necessary and sufficient rank condition in Proposition 2 holds. The parameters $\hat{\varsigma}_T$ estimated by the CMD approach are summarized in the upper panel of Table S.5, along with associated 68% MBB confidence intervals. The overidentifying restrictions test, reported at the bottom panel of Table S.5, strongly supports the estimated model with a p-value of 0.86.

The CMD estimates in Table S.5 reveal important information about the properties and quality of the instruments used to estimate fiscal proxy-SVAR. The tax instrument z_t^{tax} is poorly correlated with the tax shock ε_t^{tax} in the Great Inflation period, where the relevance parameter $\varphi_{1,1}$ is not statistically significant. However, the relevance of the tax instrument increases markedly in the Great Moderation regime, where the change parameter $\Delta_{\varphi_{1,1}}$, is significant and the overall magnitude and statistical significance of $\varphi_{1,1} + \Delta_{\varphi_{1,1}}$ become substantial. To illustrate, examining columns (ii) and (iii) of Table 3 in the text, we observe that the correlation between the tax proxy z_t^{tax} and the estimated tax shock ε_t^{tax} jumps from 15% to 45%.[2] Moreover, the 68% MBB confidence interval for the contamination parameter, υ_{tax}^{y}, suggests that the tax proxy is negatively linked, albeit not dramatically, with the output shock. A similar finding is also documented in Keweloh, Klein, and Prüser (2024), leveraging the non-normality of structural shocks in a Bayesian approach; see also Lewis (2021). Notice that the implied "contamination correlations" in Table 3, columns (ii) and (iii), vary from -13% in the Great Inflation to -11% in the Great Moderation.

(V) CHECKS OF IDENTIFIABILITY The smallest singular value of the estimated Jacobian matrix, $\mathcal{J}(\hat{\varsigma}_T)$, shown at the bottom of Table S.5 with associated 68% MBB confidence

[2]This marked change in the relevance of the narrative tax instrument is not surprising given its zero-censored nature, where the zeros tend to weaken relevance. Simple accounting shows that the number of zeros characterizing the tax instrument,z_t^{tax}, in the Great Inflation period, where volatility is higher, is considerably higher than the number of zeros in the Great Moderation.

interval, provides an informal check of the quality of the identification. While we note that the bootstrap confidence interval for the smallest singular value does not include zero, we acknowledge that this cannot be considered conclusive statistical evidence that the rank condition in Proposition 2 is satisfied. Nonetheless, we find no clear indication of identification failure due to insufficient information from the detected volatility shift.

(vi) Additional Information about the Dynamic Tax Multipliers The dynamic tax multipliers displayed in the upper panel of Figure 1 in the text display noticeable differences across the two volatility regimes. Relative to the case in which the proxy-SVAR is estimated on the entire sample ignoring the break in volatility (black solid line), we observe a significant reduction in magnitude in both volatility regimes, accompanied by a substantial reduction of estimation uncertainty.

Our estimate of the tax multiplier in column (ii) of Table 3, $\mathcal{M}_{tax}^{peak}$, peaks at 1.73 (8 quarters after the shock) during the Great Inflation and declines to a peak of 0.53 (on-impact) during the Great Moderation. However, while estimates for the Great Inflation where the tax narrative proxy weakly correlates with the tax shock are relatively precise, those for the Great Moderation, with a stronger correlation, are highly imprecise. on the Great Moderation, also the estimated output elasticity of tax revenues ϑ_y^{tax} displays a wide 68% MBB confidence interval. These results suggest two considerations. First, the peak tax multipliers obtained with the proxy-SVAR approach on the whole estimation sample (approximately 3 in Mertens and Ravn (2014) and 2.6 in our framework) may likely reflect a bias induced by not account for the shift in volatility, the change in the strength of the tax proxy across the volatility regimes and the possible, albeit modest, contamination of the tax proxy from the output shock. Second, accounting for the volatility shifts guarantees consistency of the estimates and reveals that the effect of exogenous tax shocks on output is considerably different across the two regimes considered.

Simple calculations show that the weighted average of our peak tax multipliers in the two macroeconomic regimes, using the fractions of sample observations before and after the volatility shift as weights, is approximately 1. This value is close to the peak multiplier for tax cuts of 0.86 inferred by Lewis (2021) using his identification approach based on time-varying volatility and constant IRFs, a hypothesis that our estimates call into question.

Our estimated proxy-SVAR clearly indicates that tax cuts are less effective in stimulating output during the Great Moderation compared to the Great Inflation. This finding can be explained by considering the differences in price and wage flexibility and access to credit markets in these two periods. During the Great Inflation, when prices and wages were stickier, tax cuts had stronger real effects because nominal rigidities prevented rapid price adjustments that would have otherwise offset their impact. In contrast, during the Great Moderation, more flexible prices and wages allowed the economy to adjust more quickly through price changes, partially mitigating the real impact of tax cuts. Furthermore, during the Great Inflation, when households had limited access to credit markets, tax cuts provided a vital source of immediate liquidity, leading households to spend a larger portion of their tax savings promptly, amplifying the impact on aggregate demand and output. Conversely, during the Great Moderation, with more developed financial markets and better access to credit, households could already smooth their consumption patterns through borrowing, making the effects of tax cuts less effective.

(vii) Estimated Impulse Response Functions Figure 1 in the main text displays markedly different dynamic tax multipliers across the two identified volatility regimes. We complete the analysis by plotting and briefly discussing the IRFs from the estimated model, which yield the dynamic fiscal multipliers.

Figure S.3 presents the IRFs, normalized as in Mertens and Ravn (2014) (see their Fig. 4), specifically considering a tax cut of one percentage point of GDP. The graph shows that output increases by 0.5% on impact in both regimes, albeit with considerable uncertainty. It then rises to a peak of almost 1.8% after 8 quarters in the Great Inflation regime. Output responses after 4 quarters are very precisely estimated during the Great Inflation. Conversely, the output response to the tax cut is surrounded by high uncertainty during the Great Moderation regime. Tax revenues respond markedly to the tax cut in the Great Inflation period, displaying a rebound effect after roughly 6 quarters, while responding more persistently during the Great Moderation.

Interestingly, the responses plotted in Fig. 4 of Mertens and Ravn (2014) resemble the shape of our responses under the Great Inflation. This evidence further suggests that the high tax multipliers estimated by Mertens and Ravn (2014) reflect the combined effect of two phenomena: (a) the omission of the marked decline in volatility from the Great Inflation to the Great Moderation, which probably caused a shift in how output responds to tax shocks, and (b) the fact that their estimated tax multipliers on the entire sample (ignoring the break) likely mirror the dynamic patterns specific to the Great Inflation period.

(viii) Extended model with consumer price inflation As a robustness check, we extend the baseline specification by including consumer price inflation (π_t) as the fourth endogenous variable in the fiscal VAR. The same two fiscal instruments used in the baseline model are employed to identify the two fiscal shocks. The VAR specification (number of lags and treatment of variables) is the same as in the baseline model.

The stability restrictions used for this expanded model, summarized in Equation (S.18) below, are formulated to reproduce as closely as possible the setup discussed for the baseline model. The inflation rate is allowed to respond instantaneously to all shocks in the system. However, we impose the restriction that there is no instantaneous change in the response of inflation to the output shock in the move from the Great Inflation to the Great Moderation.

The proxy-SVAR with shift in volatility presented in Equation (S.18) is overidentified (there are 39 free parameters which are estimated with 42 moment conditions) and is estimated by the CMD approach. The overidentifying restriction test is equal to 1.61, with a p-value of 0.66. The implied IRFs are plotted in Figure S.4 and the corresponding fiscal multipliers in Figure S.5. In Figure S.4 the tax shock is contractionary.

The estimated fiscal multipliers in Figure S.5 are very similar to those obtained from the baseline three-equation model.

In panel (4,2) of Figure S.4, we observe that the fiscal spending shock is inflationary during the Great Inflation, though its effects only become statistically significant several quarters after impact. On-impact responses tend to be negative but are imprecisely estimated. The fiscal spending shock also triggers consumer price inflation during the Great Moderation, but with a comparatively less pronounced effect than during the Great Inflation. Furthermore, in this latter macroeconomic regime, we do not observe the puzzling negative response of consumer price inflation in the first quarters after the shock. This

likely reflects the Federal Reserve's aggressive mandate toward stabilizing inflation during that period. For a thorough discussion of the inflationary effects of fiscal spending shocks, we refer, e.g., to Jørgensen and Ravn (2022).

$$\begin{pmatrix} u_t^{TR} \\ u_t^{GS} \\ u_t^{GDP} \\ u_t^{\pi} \\ \hline z_t^{tax} \\ z_t^{g} \end{pmatrix} = \underbrace{\left(\begin{array}{cc:c:cc} h_{1,1} & h_{1,2} & h_{1,3} & h_{1,4} & 0 & 0 \\ h_{2,1} & h_{2,2} & 0 & h_{2,4} & 0 & 0 \\ h_{3,1} & h_{3,2} & h_{3,3} & h_{3,4} & 0 & 0 \\ h_{4,1} & h_{4,2} & h_{4,3} & h_{4,4} & 0 & 0 \\ \hline \varphi_{1,1} & \varphi_{1,2} & v_{tax}^{y} & 0 & \omega_{tax} & 0 \\ 0 & \varphi_{2,2} & v_{g}^{y} & 0 & \omega_{g,tax} & \omega_{g} \end{array}\right)}_{G} \underbrace{\begin{pmatrix} \varepsilon_t^{tax} \\ \varepsilon_t^{g} \\ \hline \varepsilon_t^{y} \\ \varepsilon_t^{\pi} \\ \hline \zeta_t^{tax} \\ \zeta_t^{g} \end{pmatrix}}_{\xi_t}$$

$$+ \underbrace{\left(\begin{array}{cc:c:cc} \Delta_{h_{1,1}} & \Delta_{h_{1,2}} & \Delta_{h_{1,3}} & \Delta_{h_{1,4}} & 0 & 0 \\ \Delta_{h_{2,1}} & \Delta_{h_{2,2}} & 0 & 0 & 0 & 0 \\ 0 & \Delta_{h_{3,2}} & \Delta_{h_{3,3}} & \Delta_{h_{3,4}} & 0 & 0 \\ \Delta_{h_{4,1}} & \Delta_{h_{4,2}} & 0 & \Delta_{h_{4,4}} & 0 & 0 \\ \hline \Delta_{\varphi_{1,1}} & \Delta_{\varphi_{1,2}} & 0 & 0 & 0 & 0 \\ 0 & \Delta_{\varphi_{2,2}} & 0 & 0 & 0 & \Delta_{\omega_g} \end{array}\right)}_{\Delta_G} \mathbb{I}\left(t \geq T_B + 1\right) \underbrace{\begin{pmatrix} \varepsilon_t^{tax} \\ \varepsilon_t^{g} \\ \hline \varepsilon_t^{y} \\ \varepsilon_t^{\pi} \\ \hline \zeta_t^{tax} \\ \zeta_t^{g} \end{pmatrix}}_{\xi_t} \tag{S.18}$$

(IX) FISCAL SPENDING MULTIPLIERS As mentioned in the paper, our instrument z_t^g for fiscal spending shock is borrowed from Angelini, Caggiano, et al. (2023). This proxy is constructed by "purging" the residuals obtained from a regression of a measure of news spending shocks proposed by Ramey (2011) on a set of macroeconomic indicators. The logic behind this construction is to remove the component of the one-step-ahead fiscal spending forecast error that can be anticipated based on narrative records. Hence, the time series z_t^g does not coincide precisely with that used in Mertens and Ravn (2014) for instrumenting fiscal spending shocks. This explains why our results, obtained on the estimation sample from 1950:Q1-2006:Q4 without taking volatility change into account, do not match precisely those in Mertens and Ravn (2014). The lower panel of Figure 1 displays the dynamic fiscal spending multipliers estimated from the proxy-SVAR. Solid red lines represent the Great Inflation period, with 68% MBB confidence intervals indicated by the red shaded areas. Solid blue lines represent the Great Moderation period, with 68% MBB confidence intervals indicated by the blue shaded areas. While the dynamic tax multipliers (shown in the top panel) exhibit pronounced differences in magnitude and uncertainty across the two periods, this is not the case for the dynamic fiscal spending multipliers. The estimated peak fiscal spending multiplier, $\mathcal{M}_g^{peak}$, summarized in columns (ii) and (iii) of Table 3 is 2.40 in the Great Inflation regime and declines to 2.03 in the Great Moderation regime. These point estimates have comparable 68% MBB confidence intervals of (1.2, 2.5) and (1.3, 2.7), respectively. The only notable difference between the two volatility regimes is that the peak effect is achieved four quarters after the shock in the Great Inflation regime and two quarters after the shock in the Great Moderation regime. We observe that ignoring the volatility shift, see column (i) of Table 3, our estimate of the peak fiscal spending multiplier is comparable with the results in Caldara and Kamps (2017) obtained by estimating fiscal reaction functions and instrumenting non-fiscal shocks with non-fiscal instruments.

Interestingly, our findings on the fiscal spending multiplier diverge from those in Lewis (2021) while sharing both similarities and differences with Fritsche, Klein, and Rieth (2021). Lewis (2021), who considers the same estimation sample and a time-varying volatility approach with constant IRFs, detects a fiscal spending multiplier that peaks at 0.75 after two quarters but is estimated very imprecisely. In contrast, Fritsche et al. (2021) employ in one of their specifications Markov-switching dynamics across high- and low-volatility states, allowing IRFs to change across these states. Using an estimation sample that partially covers the period after the Global Financial Crisis, they find changes in the impact of government spending shocks between high- and low-volatility regimes, with the high-volatility state essentially matching our Great Inflation period and the low-volatility state covering our Great Moderation sample. Therefore, the main difference between their and our results can be attributed to our inclusion of the instrument z_t^g and the simultaneous identification of the tax shock. Results on estimated relevance and contamination in Table 3 suggest that z_t^g is a valid instrument. Fritsche et al. (2021) establish that the fiscal spending multiplier is significantly higher in the low-volatility state (where it peaks around 2.5–3) compared to the high-volatility state (where it peaks around 1.72–2). Our results are only partially consistent with these findings. While the magnitudes of our estimated fiscal spending multipliers are broadly comparable, we detect a larger multiplier during the Great Inflation (high-volatility state) relative to the Great Moderation (low-volatility state).

S.7 Proofs of propositions

Proof of Proposition 1 : (i) Consider the sums:

$$\hat{\Sigma}_{u,z} := \frac{1}{T}\sum_{t=1}^{T}\hat{u}_t z_t' = \frac{1}{T}\left\{\sum_{t=1}^{T_B}\hat{u}_t z_t' + \sum_{t=T_B+1}^{T}\hat{u}_t z_t'\right\}$$

$$= \frac{1}{T}\left\{\frac{T_B}{T_B}\sum_{t=1}^{T_B}\hat{u}_t z_t' + \frac{T-T_B}{T-T_B}\sum_{t=T_B+1}^{T}\hat{u}_t z_t'\right\}$$

$$= \frac{T_B}{T}\left\{\frac{1}{T_B}\sum_{t=1}^{T_B}\hat{u}_t z_t'\right\} + \frac{T-T_B}{T}\left\{\frac{1}{T-T_B}\sum_{t=T_B+1}^{T}\hat{u}_t z_t'\right\}. \tag{S.19}$$

For $T \to \infty$, using Assumptions 1-2 and conditions (4)-(5):

$$\frac{T_B}{T}\left\{\frac{1}{T_B}\sum_{t=1}^{T_B}\hat{u}_t z_t'\right\} \xrightarrow{\mathbb{P}} \tau_B^{(0)}\mathbb{E}\left[u_t z_t' \mathbb{I}\left(t \leq T_B\right)\right] := \tau_B^{(0)}\begin{pmatrix}\mathbb{E}\left[u_{1,t} z_t' \mathbb{I}\left(t \leq T_B\right)\right] \\ \mathbb{E}\left[u_{2,t} z_t' \mathbb{I}\left(t \leq T_B\right)\right]\end{pmatrix}$$

$$= \tau_B^{(0)}\mathbb{E}\left[\left\{H_{\bullet 1}^{(0)}\varepsilon_{1,t} + H_{\bullet 2}^{(0)}\varepsilon_{2,t}\right\} z_t'\right] = \tau_B^{(0)} H_{\bullet 1}^{(0)}\mathbb{E}\left[\varepsilon_{1,t} z_t'\right] = \tau_B^{(0)} H_{\bullet 1}^{(0)}(\Phi^{(0)})'; \tag{S.20}$$

furthermore,

$$\frac{T-T_B}{T}\left\{\frac{1}{T-T_B}\sum_{t=T_B+1}^{T}\hat{u}_t z_t'\right\} \xrightarrow{\mathbb{P}} (1-\tau_B^{(0)})\mathbb{E}\left[u_t z_t' \mathbb{I}\left(t>T_B\right)\right]$$

$$= (1-\tau_B^{(0)})\mathbb{E}\left[\left\{(H_{\bullet 1}^{(0)}+\Delta_{H_{\bullet 1}}^{(0)})(\Lambda_{\bullet 1}^{(0)})^{1/2}\varepsilon_{1,t}+(H_{\bullet 2}^{(0)}+\Delta_{H_{\bullet 2}}^{(0)})(\Lambda_{\bullet 2}^{(0)})^{1/2}\varepsilon_{2,t}\right\} z_t'\right]$$

$$= (1-\tau_B^{(0)})(H_{\bullet 1}^{(0)}+\Delta_{H_{\bullet 1}}^{(0)})(\Lambda_{\bullet 1}^{(0)})^{1/2}\mathbb{E}\left[\varepsilon_{1,t}z_t'\right] = (1-\tau_B^{(0)})(H_{\bullet 1}^{(0)}+\Delta_{H_{\bullet 1}}^{(0)})(\Lambda_{\bullet 1}^{(0)})^{1/2}(\Phi^{(0)})', \quad \text{(S.21)}$$

where use has been made of the following matrix decompositions: $H^{(0)} = (H_{\bullet 1}^{(0)}, H_{\bullet 2}^{(0)})$, $\Delta_H^{(0)} = (\Delta_{H_{\bullet 1}}^{(0)}, \Delta_{H_{\bullet 2}}^{(0)})$,

$$\Lambda^{(0)} = \begin{pmatrix} \Lambda_{\bullet 1}^{(0)} & \\ & \Lambda_{\bullet 2}^{(0)} \end{pmatrix}.$$

Considering (S.20) and (S.21) jointly, the result follows.
(ii) Estending the agument in (S.19) to the components $\hat{\Sigma}_{u_2,z}$ and $\hat{\Sigma}_{u_1,z}$ of $\hat{\Sigma}_{u,z}$:

$$\frac{T_B}{T}\begin{pmatrix} \frac{1}{T_B}\sum_{t=1}^{T_B}\hat{u}_{1,t}z_t' \\ \frac{1}{T_B}\sum_{t=1}^{T_B}\hat{u}_{2,t}z_t' \end{pmatrix} \xrightarrow{\mathbb{P}} \tau_B^{(0)}\begin{pmatrix} \mathbb{E}\left[u_{1,t}z_t'\mathbb{I}\left(t\le T_B\right)\right] \\ \mathbb{E}\left[u_{2,t}z_t'\mathbb{I}\left(t\le T_B\right)\right] \end{pmatrix} = \tau_B^{(0)}\begin{pmatrix} H_{1,1}^{(0)}(\Phi^{(0)})' \\ H_{2,1}^{(0)}(\Phi^{(0)})' \end{pmatrix};$$

$$\frac{T-T_B}{T}\begin{pmatrix} \frac{1}{T-T_B}\sum_{t=T_B+1}^{T}\hat{u}_{1,t}z_t' \\ \frac{1}{T-T_B}\sum_{t=T_B+1}^{T}\hat{u}_{2,t}z_t' \end{pmatrix} \xrightarrow{\mathbb{P}} (1-\tau_B^{(0)})\begin{pmatrix} \mathbb{E}\left[u_{1,t}z_t'\mathbb{I}\left(t>T_B\right)\right] \\ \mathbb{E}\left[u_{2,t}z_t'\mathbb{I}\left(t>T_B\right)\right] \end{pmatrix}$$

$$= (1-\tau_B^{(0)})\begin{pmatrix} (H_{1,1}^{(0)}+\Delta_{H_{1,1}}^{(0)})(\Lambda_{\bullet 1}^{(0)})^{1/2}(\Phi^{(0)})' \\ (H_{2,1}^{(0)}+\Delta_{H_{2,1}}^{(0)})(\Lambda_{\bullet 1}^{(0)})^{1/2}(\Phi^{(0)})' \end{pmatrix}.$$

It turns out that:

$$\hat{\Sigma}_{u_2,z}\left(\hat{\Sigma}_{u_1,z}\right)^{-1} \xrightarrow{\mathbb{P}} \tau_B^{(0)}\begin{pmatrix} 1 \\ H_{2,1}^{rel(0)} \end{pmatrix} + (1-\tau_B^{(0)})\begin{pmatrix} 1 \\ (H_{2,1}^{(0)}+\Delta_{H_{2,1}}^{(0)})(H_{1,1}^{(0)}+\Delta_{H_{1,1}}^{(0)})^{-1} \end{pmatrix}.$$

■

Proof of Corollary 1: The proof trivially follows from the proof of Proposition 1 by setting $\Delta_{H_{\bullet 1}}^{(0)} = 0_{n\times k}$. ■

Proof of Proposition 2: (i) The result follows by deriving the moment conditions (16) with respect to the parameter $\varsigma := (\gamma', \delta', \psi')'$, applying standard matrix derivative rules; (ii) the necessary order condition follows from the dimensions of the Jacobian matrix in (20). ■

Proof of Proposition 3: Let $\hat{Q}_T(\varsigma) := m_T(\hat{\sigma}_\eta, \varsigma)'\hat{V}_{\sigma_\eta}^{-1} m_T(\hat{\sigma}_\eta, \varsigma)$ be the objective function upon which CMD estimation is computed in (23). We observe that: (a) under the conditions of Proposition 2, $Q_0(\varsigma) := m(\sigma^{(0)}, \varsigma)' V_{\sigma_\eta}^{-1} m(\sigma^{(0)}, \varsigma)$ is uniquely maximized at $\varsigma^{(0)}$ in the neighborhood $\mathcal{N}_{\varsigma^{(0)}}$; (b) $\mathcal{P}_\varsigma$ is compact and $\mathcal{N}_{\varsigma^{(0)}} \subseteq \mathcal{P}_\varsigma$; (c) $Q_0(\varsigma)$ is continuous; (d) $\hat{Q}_T(\varsigma)$ converges uniformly in probability to $Q_0(\varsigma)$. To prove that (d) holds, recall that under Assumptions 1-2 $\hat{\sigma}_\eta \xrightarrow{\mathbb{P}} \sigma_\eta^{(0)}$, and $m_T(\bullet, \varsigma)$ is continuous, hence $m_T(\hat{\sigma}_\eta, \varsigma) \xrightarrow{\mathbb{P}} m(\sigma_\eta^{(0)}, \varsigma)$ by

the Continuous Mapping Theorem. Also recall that it exists an estimator of the asymptotic covariance matrix V_{σ_η} such that $\hat{V}_{\sigma_\eta} \xrightarrow{\mathbb{P}} V_{\sigma_\eta}$, see (23). Then, with $\|\cdot\|$ denoting the Euclidean norm, by the triangle and the Cauchy-Schwartz inequalities:

$$\begin{aligned}\left|\hat{Q}_T(\varsigma) - Q_0(\varsigma)\right| \leq & \left|[m_T(\hat{\sigma}_\eta,\varsigma) - m(\sigma_\eta^{(0)},\varsigma)]'\hat{V}_{\sigma_\eta}^{-1}[m_T(\hat{\sigma}_\eta,\varsigma) - m(\sigma_\eta^{(0)},\varsigma)]\right| \\ & + \left|m(\sigma_\eta^{(0)},\varsigma)'[\hat{V}_{\sigma_\eta}^{-1} + \hat{V}_{\sigma_\eta}^{-1\prime}][m_T(\hat{\sigma}_\eta,\varsigma) - m(\sigma_\eta^{(0)},\varsigma)]\right| \\ & + \left|m(\sigma_\eta^{(0)},\varsigma)'[\hat{V}_{\sigma_\eta}^{-1} - V_{\sigma_\eta}^{-1}]m(\sigma_\eta^{(0)},\varsigma)\right| \\ \leq & \left\|m_T(\hat{\sigma}_\eta,\varsigma) - m(\sigma_\eta^{(0)},\varsigma)\right\|^2 \left\|\hat{V}_{\sigma_\eta}^{-1}\right\| \\ & + 2\left\|m(\sigma_\eta^{(0)},\varsigma)\right\| \left\|m_T(\hat{\sigma}_\eta,\varsigma) - m(\sigma_\eta^{(0)},\varsigma)\right\| \left\|\hat{V}_{\sigma_\eta}^{-1}\right\| \\ & + \left\|m(\sigma_\eta^{(0)},\varsigma)\right\|^2 \left\|\hat{V}_{\sigma_\eta}^{-1} - V_{\sigma_\eta}^{-1}\right\|\end{aligned}$$

so that $\sup_{\varsigma\in\mathcal{P}_\varsigma}\left|\hat{Q}_T(\varsigma) - Q_0(\varsigma)\right| \xrightarrow{\mathbb{P}} 0$. Given (a), (b), (c), and (d), the consistency result follows from Theorem 2.1 in Newey and McFadden (1994).

To prove asymptotic normality, we start from the first-order conditions implied by the problem (23) in the paper:

$$\mathcal{J}(\hat{\varsigma}_T)'\hat{V}_{\sigma_\eta}^{-1}m_T(\hat{\sigma}_\eta,\hat{\varsigma}_T) = 0 \tag{S.22}$$

where $\mathcal{J}(\hat{\varsigma}_T)$ denotes the Jacobian matrix $\mathcal{J}(\varsigma) := \mathcal{J}(\sigma_\eta,\varsigma) := \frac{\partial m(\sigma_\eta,\varsigma)}{\partial\varsigma'}$ evaluated at the estimated parameters $\hat{\sigma}_\eta$, and $\hat{\varsigma}_T$). By expanding $m_T(\hat{\sigma}_\eta,\hat{\varsigma}_T)$ around $\varsigma^{(0)}$ and solving, yields the expression (valid in $\mathcal{N}_{\varsigma^{(0)}}$):

$$\begin{aligned}&\sqrt{T}(\hat{\varsigma}_T - \varsigma^{(0)}) \\ &= -\left\{\mathcal{J}(\hat{\sigma}_\eta,\hat{\varsigma}_T)'\hat{V}_{\sigma_\eta}^{-1}\mathcal{J}(\hat{\sigma}_\eta,\bar{\varsigma})\right\}^{-1}\mathcal{J}(\hat{\sigma}_\eta,\hat{\varsigma}_T)'\hat{V}_{\sigma_\eta}^{-1}\sqrt{T}m_T(\hat{\sigma}_\eta,\varsigma^{(0)})\end{aligned} \tag{S.23}$$

where $\bar{\varsigma}$ is a mean value. From (23) and the delta-method:

$$\sqrt{T}m_T(\hat{\sigma}_\eta,\varsigma^{(0)}) \xrightarrow{d} N(0,\mathcal{J}(\varsigma^{(0)})V_{\sigma_\eta}\mathcal{J}(\varsigma^{(0)})') \tag{S.24}$$

where $\mathcal{J}(\hat{\sigma}_\eta,\varsigma^{(0)}) \xrightarrow{\mathbb{P}} \mathcal{J}(\varsigma^{(0)}) := \mathcal{J}(\sigma_\eta^{(0)},\varsigma^{(0)})$. From the consistency result in (i), as $T\to\infty$, $\mathcal{J}(\hat{\sigma}_\eta,\hat{\varsigma}_T) \xrightarrow{\mathbb{P}} \mathcal{J}(\varsigma^{(0)})$ and $\mathcal{J}(\hat{\sigma}_\eta,\bar{\varsigma}) \xrightarrow{\mathbb{P}} \mathcal{J}(\varsigma^{(0)})$, respectively. Moreover, the matrix $\mathcal{J}(\varsigma^{(0)})'V_{\sigma_\eta}^{-1}\mathcal{J}(\varsigma^{(0)})$ is nonsingular in $\mathcal{N}_{\varsigma^{(0)}}$ because of Proposition 2. It turns out that

$$-\left\{\mathcal{J}(\hat{\sigma}_\eta,\hat{\varsigma}_T)'\hat{V}_{\sigma_\eta}^{-1}\mathcal{J}(\hat{\sigma}_\eta,\bar{\varsigma})\right\}^{-1}\mathcal{J}(\hat{\sigma}_\eta,\hat{\varsigma}_T)\hat{V}_{\sigma_\eta}^{-1} \xrightarrow{\mathbb{P}} -\left\{\mathcal{J}(\varsigma^{(0)})'V_{\sigma_\eta}^{-1}\mathcal{J}(\varsigma^{(0)})\right\}^{-1}\mathcal{J}(\varsigma^{(0)})'V_{\sigma_\eta}^{-1},$$

so that the conclusion follows from (S.24) and the Slutzky theorem. ■

Proof of Proposition S.1: See Bacchiocchi and Fanelli (2015), supplementary material. ■

References

Al-Sadoon, M. M. (2017). "A unifying theory of tests of rank". In: *Journal of Econometrics* 199.1, pp. 49–62.

Angelini, G., Caggiano, G., Castelnuovo, E., and Fanelli, L. (2023). "Are Fiscal Multipliers Estimated with Proxy-SVARs Robust?" In: *Oxford Bulletin of Economics and Statistics* 85.1, pp. 95–122.

Angelini, G. and Fanelli, L. (2019). "Exogenous uncertainty and the identification of structural vector autoregressions with external instruments". In: *Journal of Applied Econometrics* 34.6, pp. 951–971.

Bacchiocchi, E. and Fanelli, L. (2015). "Identification in Structural Vector Autoregressive Models with Structural Changes, with an Application to US Monetary Policy". In: *Oxford Bulletin of Economics and Statistics* 77.6, pp. 761–779.

Bacchiocchi, E. and Kitagawa, T. (2025). "Locally- but not Globally-identified SVARs". In: *arXiv preprint arXiv:2504.01441*.

Bai, J. (2000). "Vector Autoregressive Models with Structural Changes in Regression Coefficients and in Variance-Covariance Matrices". In: *Annals of Economics and Finance* 1.2, pp. 303–339.

Caldara, D. and Kamps, C. (2017). "The Analytics of SVARs: A Unified Framework to Measure Fiscal Multipliers". In: *The Review of Economic Studies* 84.3, pp. 1015–1040.

Carriero, A., Marcellino, M., and Tornese, T. (2024). "Blended identification in structural vars". In: *Journal of Monetary Economics*, p. 103581.

Fritsche, J. P., Klein, M., and Rieth, M. (2021). "Government spending multipliers in (un)certain times". In: *Journal of Public Economics* 203, p. 104513.

Jørgensen, P. L. and Ravn, S. H. (2022). "The inflation response to government spending shocks: A fiscal price puzzle?" In: *European Economic Review* 141, p. 103982.

Keweloh, S. A., Klein, M., and Prüser, J. (2024). "Estimating Fiscal Multipliers by Combining Statistical Identification with Potentially Endogenous Proxies". In: *arXiv preprint arXiv:2302.13066*.

Lewis, D. J. (2021). "Identifying Shocks via Time-Varying Volatility". In: *The Review of Economic Studies* 88.6, pp. 3086–3124.

Magnus, J. R. and Neudecker, H. (1999). *Matrix differential calculus with applications in statistics and econometrics*. John Wiley & Sons.

Mertens, K. and Ravn, M. (2014). "A reconciliation of SVAR and narrative estimates of tax multipliers". In: *Journal of Monetary Economics* 68.S, S1–S19.

Newey, W. K. and McFadden, D. (1994). "Chapter 36 Large sample estimation and hypothesis testing". In: vol. 4. Handbook of Econometrics. Elsevier, pp. 2111–2245.

Ramey, V. A. (2011). "Identifying Government Spending Shocks: It's all in the Timing". In: *The Quarterly Journal of Economics* 126.1, pp. 1–50.

Schlaak, T., Rieth, M., and Podstawski, M. (2023). "Monetary policy, external instruments, and heteroskedasticity". In: *Quantitative Economics* 14.1, pp. 161–200.

Staiger, D. and Stock, J. H. (1997). "Instrumental Variables Regression with Weak Instruments". In: *Econometrica* 65.3, pp. 557–586.

Stock, J. H. and Watson, M. (2018). "Identification and Estimation of Dynamic Causal Effects in Macroeconomics Using External Instruments". In: *Economic Journal* 128.610, pp. 917–948.

Table S.1: Estimated smallest singular values of the Jacobian $\mathcal{J}(\varsigma)$ with associated IQR. Full column rank condition holds.

	$corr(z_t, \varepsilon_{2t})$							
	Υ is set to 0				Υ is unrestricted			
	0.00	0.05	0.15	0.25	0.00	0.05	0.15	0.25
Sample size, relevance	Smallest singular value of $\mathcal{J}(\varsigma)$							
$T = 250$, Strong	**0.0427** [0.0136]	**0.0418** [0.0128]	**0.0395** [0.0110]	**0.0363** [0.0099]	**0.0020** [0.0008]	**0.0022** [0.0009]	**0.0028** [0.0011]	**0.0033** [0.0012]
$T = 250$, Local-To-Zero	**0.0077** [0.0025]	**0.0077** [0.0024]	**0.0076** [0.0023]	**0.0076** [0.0023]	**0.0061** [0.0017]	**0.0061** [0.0017]	**0.0058** [0.0017]	**0.0052** [0.0017]
$T = 500$, Strong	**0.0443** [0.0099]	**0.0430** [0.0094]	**0.0405** [0.0081]	**0.0374** [0.0071]	**0.0018** [0.0005]	**0.0021** [0.0006]	**0.0026** [0.0007]	**0.0032** [0.0009]
$T = 500$, Local-To-Zero	**0.0071** [0.0015]	**0.0070** [0.0015]	**0.0069** [0.0015]	**0.0066** [0.0014]	**0.0062** [0.0012]	**0.0062** [0.0012]	**0.0058** [0.0012]	**0.0051** [0.0012]
$T = 1000$, Strong	**0.0449** [0.0071]	**0.0437** [0.0069]	**0.0412** [0.0058]	**0.0378** [0.0050]	**0.0018** [0.0004]	**0.0020** [0.0004]	**0.0025** [0.0005]	**0.0031** [0.0006]
$T = 1000$, Local-To-Zero	**0.0067** [0.0010]	**0.0067** [0.0009]	**0.0066** [0.0009]	**0.0063** [0.0009]	**0.0063** [0.0008]	**0.0063** [0.0008]	**0.0058** [0.0009]	**0.0050** [0.0009]

Notes: Numbers in the table are averages of estimates obtained across N =10,000 Monte Carlo simulations, see Section S.5 for details on the design. Bold entries indicate that the magnitude of the estimated smallest singular value is greater than 2×IQR.

Table S.2: Estimated smallest singular values of the Jacobian $\mathcal{J}(\varsigma)$ with associated IQR. Full column rank condition holds. Shrinking covariance matrices, $\varrho_T = O(T^{-1/2})$.

Shrinking shifts	$corr(z_t, \varepsilon_{2t})$							
	Υ is set to 0				Υ is unrestricted			
	0.00	0.05	0.15	0.25	0.00	0.05	0.15	0.25
Sample size, relevance	Smallest singular value of $\mathcal{J}(\varsigma)$							
$T = 250$, Strong	**0.0591** [0.0131]	**0.0593** [0.0131]	**0.0638** [0.0139]	**0.0750** [0.0157]	0.0010 [0.0009]	0.0010 [0.0009]	0.0010 [0.0009]	0.0009 [0.0008]
$T = 250$, Local-To-Zero	0.0075 [0.0064]	0.0068 [0.0054]	0.0109 [0.0087]	0.0199 [0.0130]	0.0012 [0.0011]	0.0012 [0.0011]	0.0012 [0.0011]	0.0012 [0.0010]
$T = 500$, Strong	**0.0598** [0.0093]	**0.0599** [0.0093]	**0.0646** [0.0100]	**0.0760** [0.0113]	0.0005 [0.0004]	0.0005 [0.0004]	0.0005 [0.0004]	0.0005 [0.0004]
$T = 500$, Local-To-Zero	0.0040 [0.0035]	0.0037 [0.0028]	0.0086 [0.0062]	0.0185 [0.0095]	0.0006 [0.0005]	0.0006 [0.0005]	0.0006 [0.0005]	0.0006 [0.0005]
$T = 1000$, Strong	**0.0600** [0.0065]	**0.0601** [0.0066]	**0.0648** [0.0071]	**0.0754** [0.0080]	0.0003 [0.0002]	0.0003 [0.0002]	0.0002 [0.0002]	0.0003 [0.0002]
$T = 1000$, Local-To-Zero	0.0020 [0.0017]	0.0022 [0.0016]	0.0073 [0.0044]	**0.0175** [0.0069]	0.0003 [0.0003]	0.0003 [0.0003]	0.0003 [0.0003]	0.0003 [0.0003]

Notes: Numbers in the table are averages of estimates obtained across N =10,000 Monte Carlo simulations, see Section S.5 for details on the design. Bold entries indicate that the magnitude of the estimated smallest singular value is greater than 2×IQR.

Table S.3: Relative performance (MSE) of estimators of the target IRFs.

Sample size: $T = 500$	$corr(z_t, \varepsilon_{2,t})$							
	0.00		0.05		0.15		0.25	
	$IRF_{1,1}$	$IRF_{2,1}$	$IRF_{1,1}$	$IRF_{2,1}$	$IRF_{1,1}$	$IRF_{2,1}$	$IRF_{1,1}$	$IRF_{2,1}$
Panel a) Strong proxy								
Model.1	1.00	1.00	1.00	1.00	1.00	1.00	1.00	1.00
Model.2	0.88	0.86	0.96	0.96	1.43	1.51	2.40	2.72
Model.3	5.74	6.52	5.31	5.47	6.22	5.61	8.64	8.08
Model.4	11.71	10.96	11.93	11.10	12.05	11.29	12.72	11.78
Model.5	1.99	2.39	2.39	2.85	3.57	4.26	5.20	6.32
Panel b) Local-to-zero proxy								
Model.1	1.00	1.00	1.00	1.00	1.00	1.00	1.00	1.00
Model.2	1.01	1.01	1.02	1.02	1.36	1.34	3.07	3.03
Model.3	0.99	0.99	0.99	0.99	1.00	0.99	1.00	1.00
Model.4	11.27	10.63	11.33	10.65	11.25	10.59	11.25	10.73
Model.5	9.83	11.72	10.25	13.26	9.10	14.67	8.66	14.97

Notes: Results are based on N =10,000 Monte Carlo simulations. The DGP is presented in (S.14). Model.1 denotes results obtained by the stability restrictions approach discussed in the paper. Model.2 is the same as Model.1 with the contamination parameters in υ and Δ_υ set to zero, i.e., imposing proxy exogeneity. Model.3 denotes results obtained by the change in volatility approach alone, i.e., without including the instrument. Model.4 denotes results obtained by the proxy-SVAR-H approach, see Proposition 2.(iii), i.e., assuming that the target IRFs remain constant across the two volatility regimes. Model.5 denotes results obtained by the external instrument alone, i.e., ignoring the volatility break. Numbers in the table correspond to measures of relative performance in the estimation of target IRFs based on Mean Squared Error (MSE), as discussed in Section S.5. Model.1 is used as a benchmark in the comparison; thus, relative performance measures are set to 1 for this model.

Table S.4: Rejection frequencies of the overidentifying restrictions test (5% nominal).

		$corr(z_t, \varepsilon_{2,t})$							
		ψ is set to 1				ψ is unrestricted			
		0.00	0.05	0.15	0.25	0.00	0.05	0.15	0.25
Sample size	Relevance	Rejection frequency (5%)							
$T = 250$	Strong	10.05	10.20	10.30	10.61	3.97	4.11	4.10	4.29
	Local-to-zero	10.17	10.08	10.15	9.81	3.94	4.02	3.90	4.02
$T = 500$	Strong	19.82	19.54	19.71	19.40	4.68	4.60	4.92	4.63
	Local-to-zero	19.77	19.48	18.96	19.27	4.55	4.87	4.75	4.97
$T = 1000$	Strong	38.04	38.40	38.71	38.49	4.71	4.96	5.01	5.22
	Local-to-zero	38.38	38.46	38.49	38.32	4.94	4.86	4.88	5.08

Notes: Rejection frequencies are computed across N =10,000 Monte Carlo simulations. The DGP is presented in Equation (S.14). Estimates of proxy-SVAR parameters are obtained by the CMD approach discussed in Section 2.4.2.

Table S.5: Estimated parameters of the fiscal proxy-SVAR with a shift in volatility at time T_B = 1983:Q2, and associated 68% MBB confidence intervals (in parentheses).

	G		Δ_G
$h_{1,1}$	0.020 (0.012,0.024)	$\Delta_{h_{1,1}}$	−0.005 (−0.011,0.000)
$h_{2,1}$	−0.000 (−0.001,0.000)	$\Delta_{h_{2,1}}$	0.000 (−0.000,0.001)
$h_{3,1}$	−0.002 (−0.002,0.001)		
$h_{1,2}$	0.003 (0.000,0.006)	$\Delta_{h_{1,2}}$	−0.003 (−0.006,0.000)
$h_{2,2}$	0.014 (0.012,0.014)	$\Delta_{h_{2,2}}$	−0.007 (−0.007,−0.005)
$h_{3,2}$	0.003 (0.002,0.004)	$\Delta_{h_{3,2}}$	−0.002 (−0.002,−0.001)
$h_{1,3}$	0.018 (0.012,0.019)	$\Delta_{h_{1,3}}$	−0.007 (−0.011,−0.004)
$h_{3,3}$	0.009 (0.008,0.009)	$\Delta_{h_{3,3}}$	−0.005 (−0.006,−0.005)
$\varphi_{1,1}$	0.021 (−0.010,0.036)	$\Delta_{\varphi_{1,1}}$	0.047 (0.006,0.088)
$\varphi_{1,2}$	−0.011 (−0.018,0.003)	$\Delta_{\varphi_{1,2}}$	−0.005 (−0.023,0.012)
$\varphi_{2,2}$	0.014 (0.012,0.014)	$\Delta_{\varphi_{2,2}}$	−0.006 (−0.007,−0.005)
v^y_{tax}	−0.018 (−0.030,−0.005)		
v^y_g	0.000 (−0.000,0.000)		
ω_{tax}	0.133 (0.096,0.136)		
$\omega_{g,tax}$	−0.000 (−0.000,−0.000)		
ω_g	0.004 (0.003,0.004)	Δ_{ω_g}	−0.003 (−0.003,−0.001)

Overidentifying restrictions: 0.744 [0.863]

Min. singular value: 1.018e-6
(2.566e-7,1.021e-6)

Notes: Upper panel: CMD estimates (Section 2.4.2). Lower panel: overidentifying restrictions test with associated p-value (in brackets). Minimum singular value of the estimated Jacobian matrix $\mathcal{J}(\hat{\varsigma}_T)$ with associated 68% MBB confidence interval.

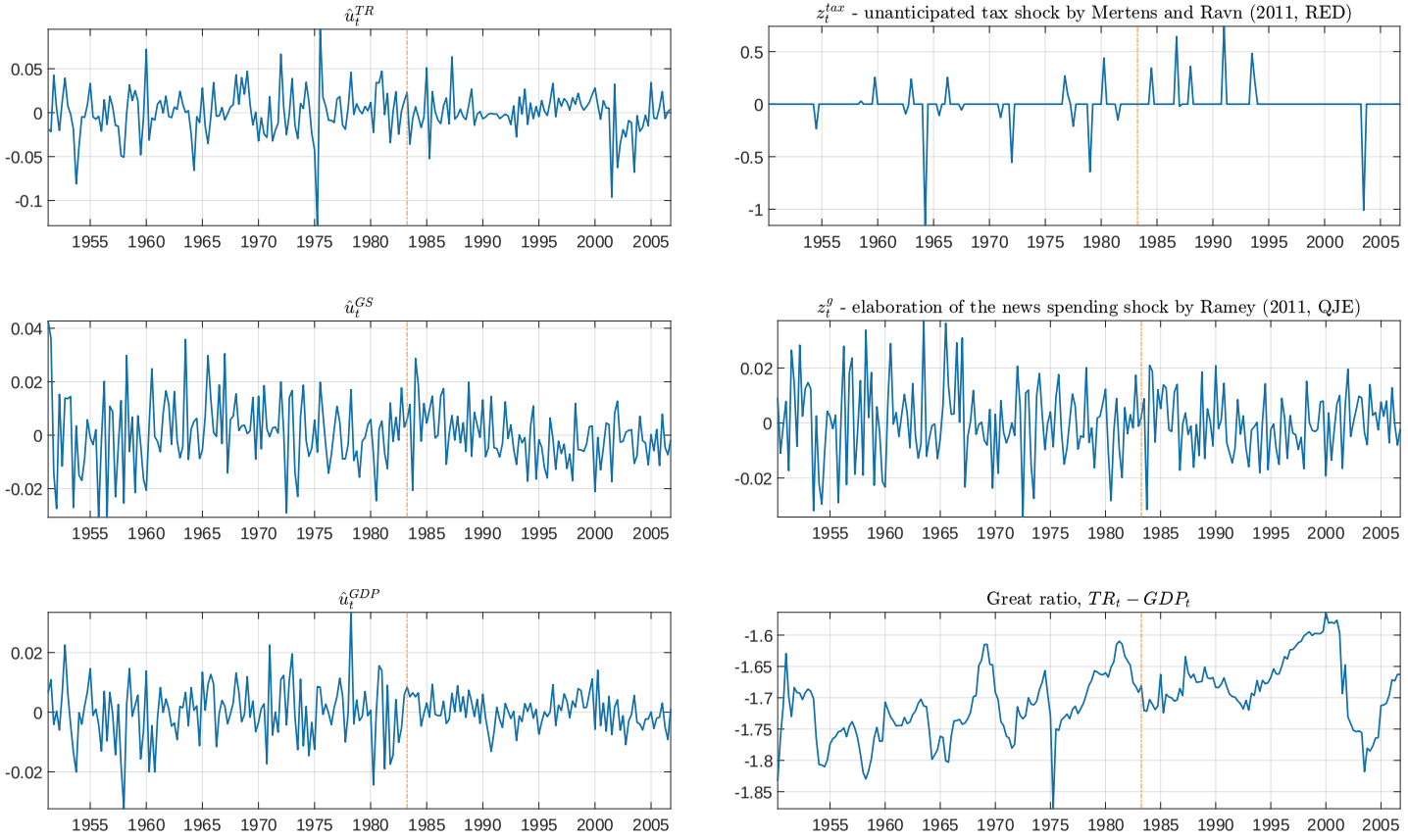

Figure S.1: Left panel: reduced form residuals of the three-equation VAR model for the variables $Y_t := (TR_t, GS_t, GDP_t)'$ estimated on the period 1950:Q1–2006:Q4. The VAR includes $p = 4$ lags. Right panel from top to bottom: Mertens and Ravn (2014)'s series of unanticipated tax shock (z_t^{tax}); series of unanticipated fiscal spending shocks (z_t^g); great ratio $TR_t - GDP_t$.

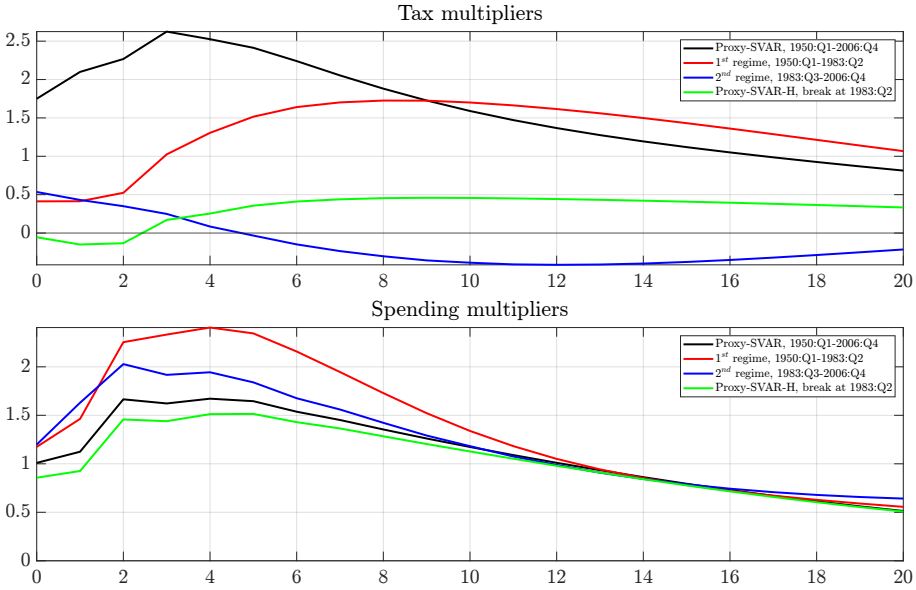

Figure S.2: Estimated dynamic fiscal multipliers without confidence intervals at a 20-quarters horizon. Tax multipliers are in the upper panel; fiscal spending multipliers in the lower panel. Black solid lines refer to multipliers estimated on the whole sample 1950:Q1–2006:Q4, without accounting for a break in volatility. Red solid lines refer to multipliers estimated on the first volatility regime 1950:Q1–1983:Q2 (Great Inflation). Blue solid lines refer to multipliers estimated on the second volatility regime 1983:Q3–2006:Q4 (Great Moderation). Green lines refer to multipliers obtained from the proxy-SVAR-H approach (see Proposition 2.(iii)), i.e. accounting for a volatility shift while maintaining regime-invariant IRFs.

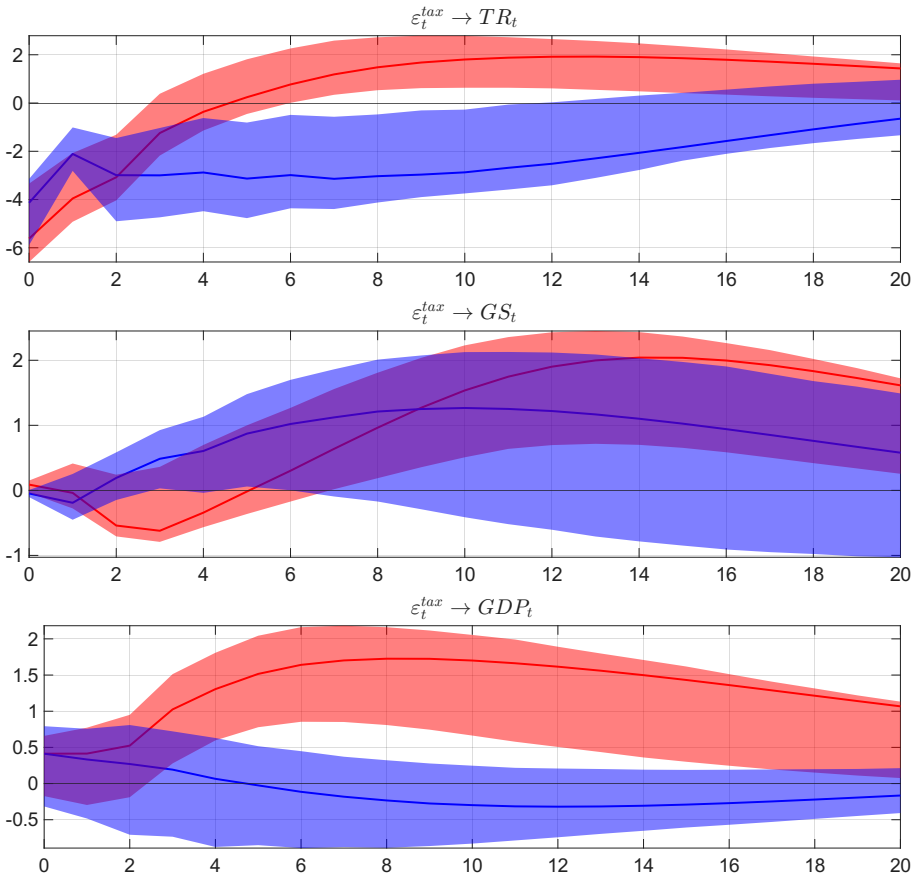

Figure S.3: Estimated IRFs to a tax cut of 1% of GDP with 68% MBB (pointwise) confidence intervals at a 20-quarters horizon response. Red solid lines refers to the IRFs estimated on the first volatility regime 1950:Q1–1983:Q2 (Great Inflation); red shaded areas are the associated 68% MBB confidence intervals. Blue solid lines refer to the IRFs estimated on the second volatility regime, 1983:Q3–2006:Q4 (Great Moderation); blue shaded areas are the associated 68% MBB confidence intervals.

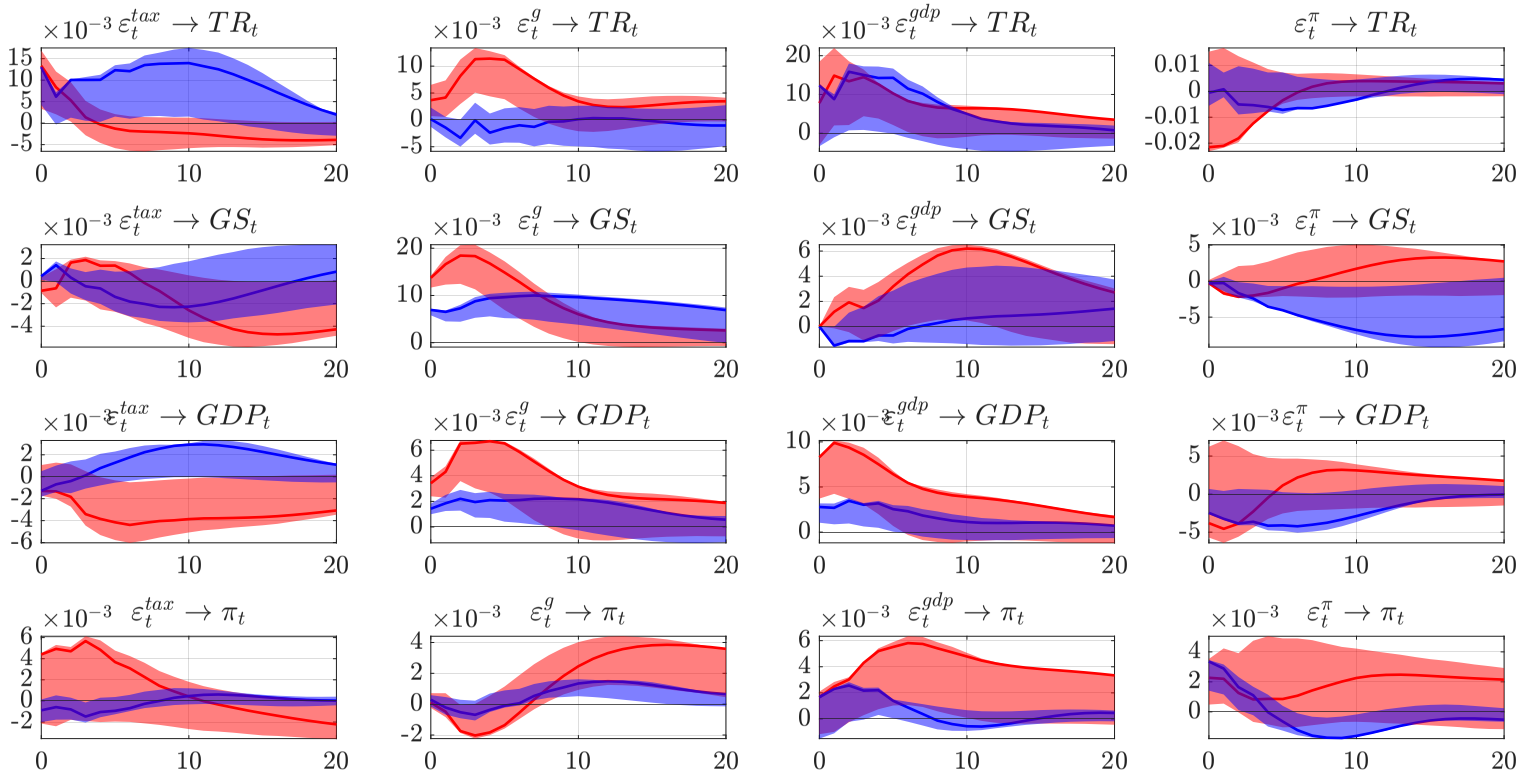

Figure S.4: Estimated IRFs with 68% MBB (pointwise) confidence intervals at a 20-quarters horizon. Results refer to the extended model with consumer price inflation. The first column shows the responses to a contractionary tax shock. Red solid line refer to IRFs estimated on the first volatility regime 1950:Q1–1983:Q2 (Great Inflation); red shaded areas are the associated 68% MBB confidence intervals. Blue solid lines refer to IRFs estimated on the second volatility regime, 1983:Q3–2006:Q4 (Great Moderation); blue shaded areas are the associated 68% MBB confidence intervals. N.B.: the first column reports IRFs to a contractionary tax shock.

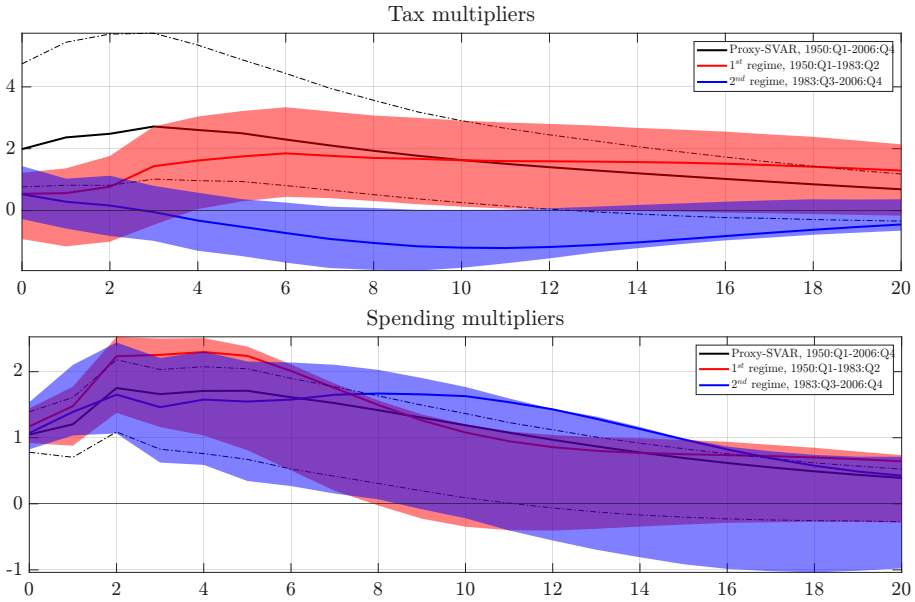

Figure S.5: Estimated dynamic fiscal multipliers with 68% MBB (pointwise) confidence intervals at a 20-quarters horizon. Tax multipliers are in the upper panel; fiscal spending multipliers in the lower panel. Results refer to the extended model with consumer price inflation. Black solid lines refer to multipliers estimated on the whole sample 1950:Q1–2006:Q4, without accounting for the detected shift in volatility; dotted thin black lines are the associated 68% MBB confidence intervals. Red solid line refer to multipliers estimated on the first volatility regime 1950:Q1–1983:Q2 (Great Inflation); red shaded areas are the associated 68% MBB confidence intervals. Blue solid lines refer to multipliers estimated on the second volatility regime, 1983:Q3–2006:Q4 (Great Moderation); blue shaded areas are the associated 68% MBB confidence intervals.